The Study of Carbon Nanotube based Chemi-resistive Portable Biosensors used for the Detection of Bacteria

by

Gaganprit Gill

A thesis
presented to the University of Waterloo
in fulfillment of the
thesis requirement for the degree of
Master of Science
in
Chemistry

Waterloo, Ontario, Canada, 2017

Authors Declaration

"I hereby declare that I am the sole author of this thesis. This is a true copy of the thesis, including any required final revisions, as accepted by my examiners.

I understand that my thesis may be made electronically available to the public."

Abstract

The successful fabrication and characterization of a portable, disposable single walled carbon nanotube biosensor used for the detection of bacteria was demonstrated by this work. The Si/SiO_2 based SWNT growth using chemical vapor deposition techniques successfully developed ultra sensitive thin single walled carbon nanotubes. The SWNTs were transferred to a portable disposable platform, to demonstrate the commercial potential of a SWNT biosensor that is capable of sensing bacteria. The platform was developed to understand the effects of pH sensing, followed by bacteria sensing. The dominant mechanism of sensing for these devices with respect to pH sensing is chemical doping however the sensing mechanism for bacteria detection is undetermined. Using electrochemical impedance techniques to deeply understand and investigate the electrochemical changes to the surface of the SWNT sensors, the resistance change for pH sensing and bacteria sensing was concluded. With an increase in pH levels, the total resistance of the SWNT sensor also increases. The limit of detection for bacteria sensing with this platform was 10^5 cfu/mL. It was determined that the charge transfer resistance of the SWNT increases with an antibody surface immobilization and then further increases with the addition of bacteria binding to antibody. From bare electrode to antibody and then bacteria, the charge transfer resistances were 774Ω, 1025Ω, and 1229Ω, respectively. The double layer capacitance for these sensors indicated a different pattern. Preliminary results for concentrations lower than 10^5cfu./mL suggests an increase in double layer capacitance with an increase in analyte concentration. Using SWNTs as the transducing element of chemiresistive biosensors allowed for a further understanding of the electrochemical mechanisms of sensing, as well as successfully fabricating a sensitive, real-time, reproducible electrical bacteria-sensing device.

Acknowledgements

First and foremost, I would like to thank my supervisor Dr. Shirley Tang for the constant support, patience and encouragement throughout my graduate studies. My time in her lab as a Masters level student will always be appreciated. I would also like to thank my committee members Dr.Juewen Liu and Dr. Vivek Maheshwari. I sincerely appreciate their time, guidance and patience throughout my Masters journey.

I would like to thank all of the past and present members of the Tang Nanotechnology lab including Louis Cheung, Mike Coleman, Zhi Li, Andrew Ward, Yverick Rangom, Yael Zilberman, Yun Wu, Kai Wang, and Andrew Wenger. I would like to especially thank Irfani Ausri for the constant supply of bacteria when needed even during her own busy schedule. All the time she took out to make sure I had what I needed is one of the reasons this project was a success. I would like to thank Dr. Linda Nazar for allowing me to work in her lab.

I would also like to give a shout out to everyone that was involved in this journey with me outside of school. Your constant support kept me motivated and pushed me through to the end. I couldn't have done it without you all.

Table of Contents

List of Figures

List of Tables

List of Abbreviations

AFM- Atomic force microscope
AC- Alternating Current
BSA- Bovine Serum Albumin
CVD- Chemical Vapor Deposition
CNT- Carbon Nanotube
CNTTF- Carbon Nanotube Thin Film
DC- Direct Current
DI H_2O- De-ionized Water
EIA- Electrophoretic Immunoassay
EIS- Electrochemical Impedance Spectroscopy
ELISA- Enzyme Linked Immunosorbent Assay
FET- Field Effect Transistors
HF- Hydrofluoric Acid
NSB- Non-specific Binding
PBS- Phosphate Buffered Saline
PB- Phosphate Buffer
PDMS- Polydimethylsiloxane
PET- Polyethylene Terephthalate
PMMA- Poly(Methyl Methacrylate)
QNC- Quantum Nano Center
SEM- Scanning Electron Microscope
SiO_2- Silicon Dioxide
SWNT- Single Walled Carbon Nanotube
SWNTTF- Single Walled Nanotube Thin Film
UV- Ultraviolet

Chapter 1: Introduction to Biosensors

1.1. Biosensors

From the diagnosis of life-threatening diseases to detection of biological agents in warfare of terrorist attacks, biosensors are becoming a critical part of modern life.[1] Biosensor short for "Biological Sensor" is an analytical device that has the ability to convert a biological response into an electrical response. Achieving immediate detection and quantification at sub-nanomolar (nM) concentrations of specific biomolecules, such as proteins, nucleic acids, and specifically pathogens are highly sought for the progress in the field of analytical chemistry. Monitoring of low concentrations of pathogens, allows for early detection of very harmful species in an individual's system. Sensors capable of this could significantly decrease the turnaround time required for establishment and in turn limit the amount of time a pathogen has to reside and become harmful within an individual's system. Fundamentally, the true early detection of harmful species is of utmost importance as it can save the lives of thousands of individuals around the world whom suffer from diseases caused by the intake of harmful pathogens such as Escherichia coli. Current methods used for the detection of biomolecules include enzyme-linked immunosorbent assay (ELISA) and electrophoretic immunoassay (EIA). These methods require long incubation times, complicated instrumentation, sample enrichment and large sample volume, all which will require trained professionals due to complexity.[2] With the inability of true early detection of biomolecules from these conventional techniques, the next logical step is to fabricate and implement a sensitive and specific, real-time point of care pathogen detection device.

A key goal of modern science is to monitor biomolecular interactions with high sensitivity in real time, with the ultimate aim of detecting single-molecule processes in natural samples.[3-5] A review of literature shows a number of practical biomolecule-detection methods that can sense molecules such as DNA, proteins but only a few methods have actually achieved this goal. To date, the leading techniques that are capable of direct detection of biomolecule capture events include Whispering-gallery microlasers,[6-8] Micro-ring resonators,[9,10] silicon nanowire filed effect transistors (FETs),[11-13] Polymer nanowires,[14,15] and Surface plasmon resonance (SPR).[16-18] These methods have proven to be extremely sensitive, however the detection equipment, complex data analysis, and multiple steps prior to capture events, greatly hinders their point-of care capabilities.

Similarly, pathogen detection methods are currently few but, due to the involvement of many different techniques between sample preparation (extraction and purification, enrichment, separation) and analysis, they are also rich in complexity.[19] Conventional methods in this case are also used despite their long turnover time because of their high sensitivity and selectivity. Literature and **figure 1.1** below shows that the most popular methods for pathogen detection, thus far, are those based on culture and colony counting methods and polymerase chain reaction (PCR). Culture and colony counting methods are much more time consuming than PCR but both provide conclusive and unambiguous results.[19] Biosensor technology comes with promises of equally reliable results in much shorter times, allowing for real-time and point of care detection of pathogens and this is where electrical biosensors have their greatest advantage.

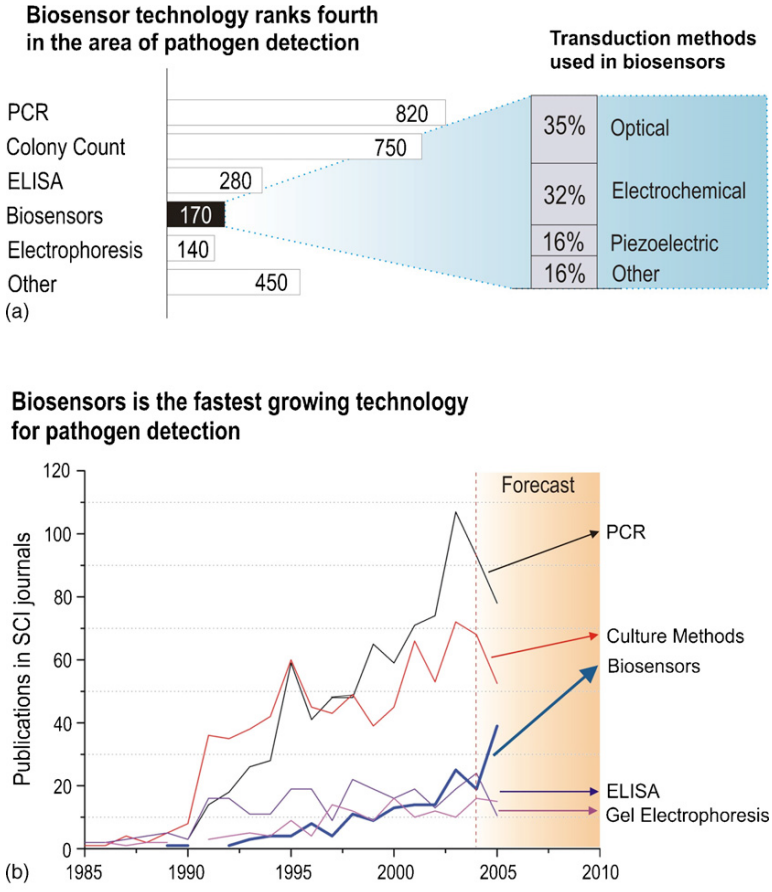

Figure 1.1: (a) Approximate number of articles using different techniques to detect and/or identify pathogen bacteria (2500 articles over past 20 years) not including articles using more than one technique. (b) Time series of the number of works published on detection of pathogen bacteria over past 20 years. Adapted from ref. 19.

1.1.1. Electrical Biosensors

Currently, as represented in **figure 1.1** most of the diagnostic assays are based on optical measurements. Utilization of nanomaterials (i.e. quantum dots and nanoparticles) can significantly improve limits of detection of such techniques. However, complicated readout instrumentation, long duration for sample preprocessing and the need for labeling make optical methods expensive, time-consuming and non-portable. In contrast, electrical detection methods rely on much simpler instrumentation that ensures lower cost, portability, and ease of use. Hence, electrical methods are ideally suitable for implementation of label-free detection approaches. Real-time and sensitive electrical detection of molecules was brought closer to realization when the first silicon based ion sensitive field effect transistor (ISFET), used for measuring ion concentrations in solution, was studied by Bergveld in 1970.[20] However, when the ISFET was first developed, theoretical studies indicated that a limit exists to the overall sensing capabilities. These biosensors were only able to achieve micromolar (μM) levels of detection. Although this is ultimate for some types of bio sensing, such as glucose levels in blood, there are many other biomolecules of interest that are functional at lower concentrations.[21] Due to this set back of non-ideal limits, extensive research regarding one-dimensional electrical biosensors has emerged over the past decade.[22] With ultra-sensitivity and specificity, and lab-on-chip capabilities, electrical biosensors have risen above conventional biomolecule detection methods as the ideal candidate for modern medicine.[23]

Electrochemical methods of detection are based on electrochemical processes that take place on the electrode surface. In order for an electrical biosensor to sense an electric signal in real-time, there are two main components that work in conjunction with each other to have a functionalized hybrid system. The first component of the system is called the receptor, typically played by a biomaterial such as a protein or nucleic acid, that recognizes a target analyte. The second component is the transducer, which converts the electrochemical changes in the local environment into an electrical signal with high sensitivity and minimal disturbance. The materials used for these components is what dictates the properties of the device such as sensitivity, selectivity and sensing time, and therefore are the most important part of an electrochemical biosensor. Depending on the transducer used, will determine the type of biosensor being developed. For electrical and electrochemical, they can be amperometric, potentiometric, or impedance-based.[24] Biosensors and biosensor test formats can be classified into *labeled* and *label-free* types depending on whether the analyte is labeled

or not. Common labels include enzymes, nanoparticles, and fluorescent probes.[24] **Figure 1.2** is a schematic representation of the typical set up of a two-terminal single walled carbon nanotube thin film electric biosensor. This electric biosensor utilizes carbon nanotubes as the key component of the transducer. The sensitivity of the biosensor depends a lot on the characteristics of the transducer (shape, type of the material, size). High surface-to-volume ratio of the transducing element can increase the efficiency of the signal being transferred, allowing for the possibility of a much more ideal limit of detection. Thus, because of the exceptional properties of carbon nanomaterials, **figure 1.2** utilizes single walled carbon nanotube thin films as the model component of the transducer.

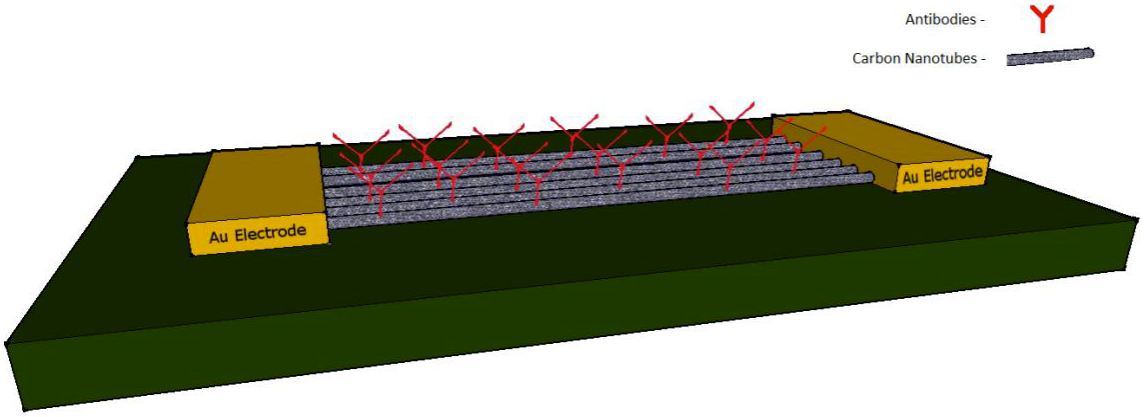

Figure 1.2: Device configuration of an electrical biosensor with SWNTTF channels layered with antibodies between two gold (Au) electrodes. Adapted from ref. 21

Figure 1.2 is a true representation of the simplicity of an electrical biosensor. With patterned transducing elements between two gold electrodes and receptors anchored onto their surface, *sensitive* and *selective* sensors can be recognized. Frequently used transducing elements for electrical biosensors include polymeric and silicon nanowires, however they can only be fabricated to as a low as 10nm in diameter. [25] This is an indication that they are not capable of achieving diffusion properties that are unique to one-dimensional nanomaterials such as single walled carbon nanotubes.[21, 26-28] However, using 0.7nm-2.5nm diameter SWNTs as the transducing component will take advantage of the unique one-dimensional diffusion properties. Many recent biosensors, particularly electrochemical biosensors have incorporated carbon nanomaterials such as SWNT as sensing elements due to their unique physical and chemical properties.[29] These properties, their fabrication process and their incorporation in electrical biosensors will be discussed anon.

To this date, there are many different techniques that can be used to fabricate SWNT based electrical biosensors. SWNTs can be transferred on to the surface of the electrodes following synthesis, or they can be grown directly between electrodes via catalyst patterning coupled with chemical vapor deposition (CVD). Depending on the specific needs of the transducing component, research groups have been able to produce a single-SWNT between electrodes[30] and single walled carbon nanotube thin films (SWNTTFs) grown between electrodes.[31] SWNTs have also been produced via non-growth, which include a SWNT surfactant solution filtration followed by soft lithography for transfer into the device[32] and alternating current electrophoresis while running a SWNT-surfactant solution through a microfluidic channel.[33]

Regardless of the fabrication process, subsequently, to the fabrication of the electrical component, the device is exposed to a specific concentration of receptor molecules, which are anchored onto the surface of SWNTs through either physical absorption or covalent binding to defect sites.[34] The success of these two different components integrated into a working device allows for the exploitation of two very unique materials working in unification, making the sensors capable of capturing and sensing a target analyte.

The ability of biomolecules to bind to a target analyte with high specificity is one of the main reasons as to why there has been such a large push in creating electrically based biosensors. Literature review shows that there are many different types of biomolecules that have the ability to selectively bind to target analyte due to their unique primary, secondary, or tertiary structure. These interactions can be seen throughout nature during nucleic acid synthesis where single stranded DNA binds to its complimentary strand and protein-protein interactions where an antibody recognizes its antigen in a system. To this date, SWNT based electric sensors have demonstrated ultralow limit of detection levels for over a diversity of analytes. For example, SWNT based platforms have boast a limit of detection of 10^5 cfu/mL for E. coli O157:H7,[35] a limit of 10^2 PFU/mL for MS2 bacteriophage,[35] 100fM limit of detection for nucleic acids[36] and fM limit of detection for H1N1 virus.[37] In previous work, our group has also demonstrated SWNTTF offering a limit of detection of 1pM in real time for M13 bacteriophage.[21] These numbers alone indicate the infinite possibilities of these electrical biosensors. This realization is also what led to the increase in study of sp^2 hybridized one-dimensional transducer electrical biosensors. Recent studies show the fabrication process of new bacteria sensing techniques to be very sensitive, however, SWNTTF based electrical

sensors have proven to acquire an advantage, as they are capable of sensitive, reproducible and real-time detection without the use of highly complicated techniques for their synthesis.

1.2. Carbon Nanomaterials for Biosensing

SWNTs have become the subject of intense investigation and have been at the forefront for the development of biosensors since their discovery.[38-42] SWNTs are derived from carbon, an element that is known to be the most versatile on the periodic table, based on the type of bonding, strength, and number of bonds it can form with many different elements. It is the chemical genius of carbon that allows it to bond in many different ways in order to create structures with entirely different properties, both at the macroscopic and nanoscopic scales. The secret behind these unique properties lies in the different hybridization that the carbon atom can undertake. Graphite and Diamond are two solid phases of pure carbon that can confirm the relevance of hybridization to the properties of these carbon-based materials. When a carbon atom shares four valence electrons equally, it is said to be sp^3 hybridized, which creates an isotropically strong diamond.[43] Diamond, a material with extreme mechanical properties, exhibits one of the strongest hardness values, has an extremely high thermal conductivity, and is an electrical insulator with a band gap of ~5.5 eV.[44] It possesses a three-dimensional cubic lattice with a lattice constant of 3.57 Å and a C-C bond length of 1.54 Å.[44] In contrast, when only three of the four groups are shared covalently between neighboring planes, and the fourth is delocalized amongst all atoms, the carbon is said to be sp^2 hybridized, also known as graphite.

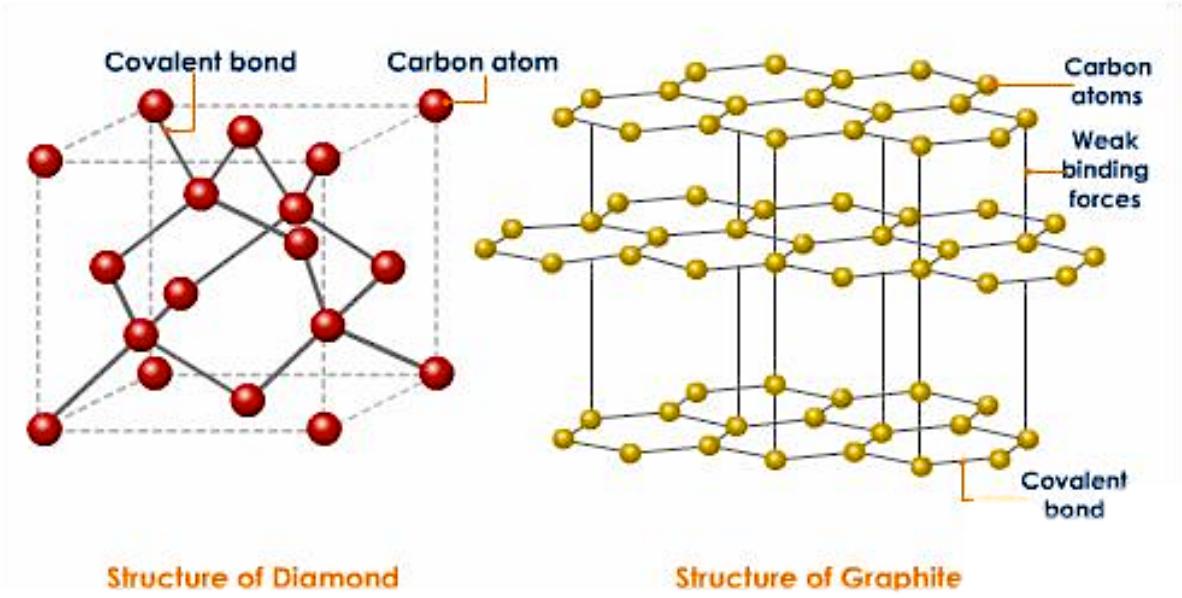

Figure 1.3: Carbon structures exhibiting different hybridizations. Sp^3 hybridized diamond (left) and sp^2 hybridized graphite (right). Adapted from ref. 44.

Graphite is the most thermodynamically stable form of carbon at room temperature comprised of a layered two-dimensional structure where each layer consists of a hexagonal honeycomb structure of sp^2 hybridized carbon atoms with a C-C bond length of 1.42 Å.[45] Single atom thick layers known as graphene layers, bond via noncovalent van der Waals forces. These weak interactions between layers of graphite indicate that the single graphene layers can be chemically or mechanically exfoliated. A graphene sheet can be conceptually rolled or distorted into other sp^2 hybridized carbon nanostructures such as SWNTs and fullerenes.

In the field of nanotechnology, carbon is very important due to the existence of 0D (fullerenes), 1D (carbon nanotubes) and 2D (graphene) nanomaterials which have unique physical and chemical properties and are promising in a number of applications. With nanometer-scale dimensions, the properties of carbon nanomaterials are not only dependent on their atomic structures, but also on their interactions with other materials. With their ability to form any shape or size, 1D SWNTs have also attracted significant attention because of their ability to withstand high temperatures, their sensitive electronic properties, their high mechanical strength, and enhanced optical and chemical assets. With the advances in producing highly mono-disperse SWNT samples renewed interest as the basis of electronic optoelectronic, and sensing applications.

1.2.1. SWNTs as Transducing Element

Carbon Nanotubes first discovered by Ijima in 1991[46] can be visualized as a piece of carbon sheet rolled into a tube like structure. Each SWNT can also be viewed as a cylinder that has a single sheet of graphite (graphene) as its surrounding wall. Based on the direction that the graphene sheet is rolled, the electrical and optical properties of the SWNT are defined. To briefly describe the geometry of SWNTs one can use lattice vectors a_1 and a_2 and indices *n, m* as shown in **figure 1.4**. The lattice vector can then be defined as:

$$C_h = n_{a_1} + m_{a_2} = (n, m) \text{ where } 0 \leq | m | \leq n \qquad \text{Equation 1}$$

The length of the chiral vector C_h is directly related to the diameter of the nanotube. The chiral angle θ between C_h and zigzag direction of the lattice *(n,* 0) is related to the indices *n, m.*[47] Nanotubes where *n=m* (θ= 30°) is referred to as armchair nanotubes because of their characteristic cross-sectional shape. Nanotubes where *m*=0 (θ = 0) are called zigzag tubes. Lastly, nanotubes that have a configuration where $n \neq m$ ($0 < \theta < 30°$) are termed chiral.[48]

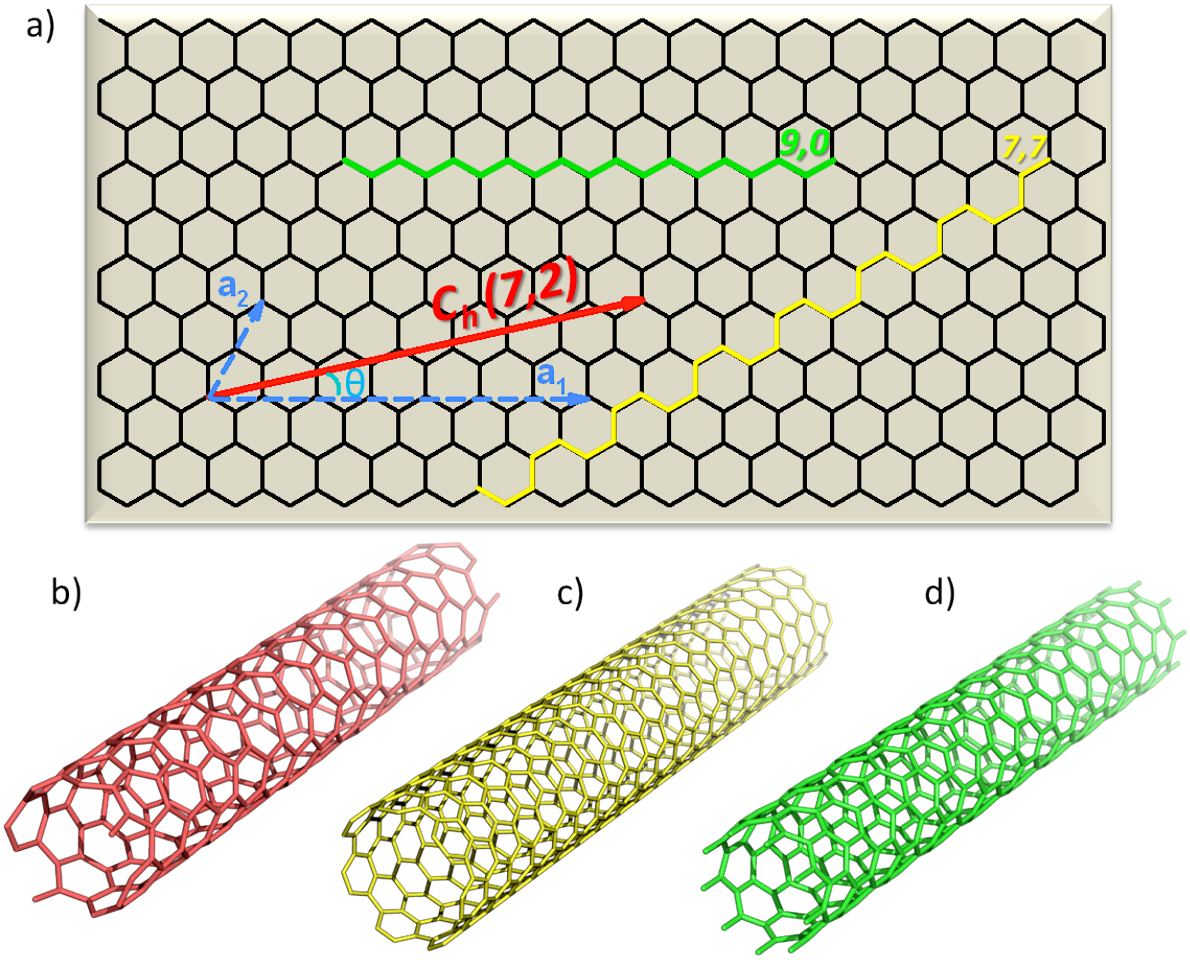

Figure 1.4: Physical structure of SWNTs. a) Yellow and green lines represent armchair and zigzag configurations respectively. C_h is the chiral vector defined by unit vectors a_1 and a_2 and angle θ. b) Chiral SWNT- (7,2), c) Armchair SWNT- (7,7) and d) Zigzag SWNT (9,0). Adapted from Ref. 24.

SWNTs as mentioned have been at the forefront for the development of biosensors since their discovery. They have popular transducing elements for electrical biosensors because of their exceptional sensitivity to the immediate environment.[49] This sensitivity to the immediate environment is due to the carbon atoms within the nanotube that are located on the modules surface, which allows for all atoms along the length of the nanotube to be affected by modifications on the surface.[50] The large surface area and molecular shape available for biomolecule interactions is the key behind enhancing the overall sensitivity of biosensors, but that's not all. The diverse range of SWNTs electrical properties is another reason why they are very attractive as the transducing element of biosensors. They display metallic or semi-conducting properties, which are highly dependent on the way SWNTs, are grown. For example, semiconducting SWNTs are promising channel materials in field-effect

transistors (FETs), whereas metallic SWNTTFs are potentially useful as transparent conductors.[51-52] As mentioned, a way to visualize SWNTs after synthesis, is to see it as a rolled up sheet of graphene. This leads to the understanding that they also exhibit similar properties to graphene in terms of band structure and density of states (DOS) as shown in **figure 1.5**. However due to boundary conditions, SWNTs hold a difference in energy level quantization as a consequence of their one-dimensional geometry.[53] An individual SWNT is therefore able to exhibit either semiconducting or metallic properties whereas graphene sheets are always zero-band gap semiconductors.

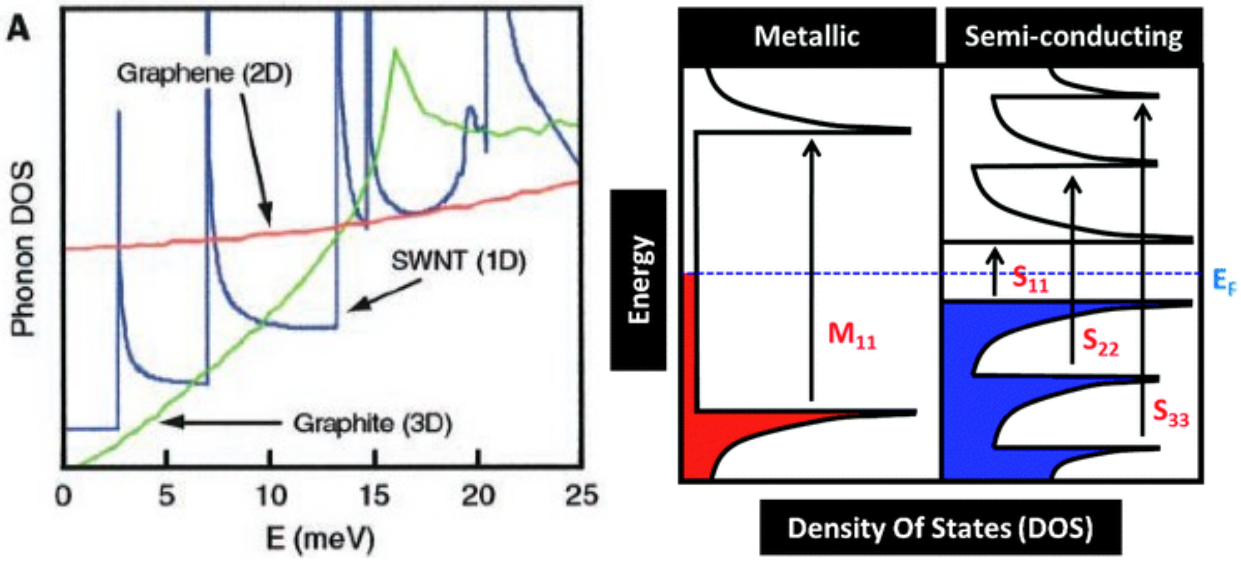

Figure 1.5: Overall density of state for 2D graphene is higher than that for a nanotube or a 3D graphite sheet (left). The right image on the right is a schematic representation of the density of states for metallic vs. semiconducting nanotubes.[51]

In a typical two-terminal setup, the overall conductance of a SWNT is tuned by the chemical interactions that occur in vicinity to their surface. A sensitive transducing component will require a low DOS around its Fermi level, which results in a material being more sensitive to energy changes caused by electrochemical interactions. This concludes that semiconducting SWNTs as the transducing element is ideal, where as metallic SWNTS do not exhibit these increased sensitivity properties due to their DOS being constant at the Fermi level (**figure 1.5**).

As mentioned, SWNTs can be produced using a variety of methods both through non-growth and growth. Some growth methods include CVD, laser ablation and arc discharge.[54] The resulting product contains a mixture of CNTs, catalyst particles, and amorphous carbon.

Additionally, the nanotubes in the mixture are not identical. They have different lengths and chiralities and thus dissimilar properties. Based on the SWNT hexagonal building block orientation and their quantized wave vector values, metallic and semiconducting SWNTs are typically synthesized at a 1:2 ratio.[55-57] Due to these limitations, modifying the synthesis and growth of our nanotubes as well as device design plays a big role in achieving favorable reproducibility and device performance. These modifications will be discussed in detail in chapter two of this thesis.

SWNTs have high aspect ratios, high mechanical strength with a young's module of 2 tetrapascal,[58] high surface areas, rich electronic properties and excellent thermal and chemical strength.[59] However, SWNTs are not very reactive due to their high-graphitized nature. Oxidation of the tubes was first shown at high temperatures (above 750°C) in the gas phase, which resulted in the formation of three functional groups: a carbonyl group (-CO), a hydroxyl group (-COH) and a carboxyl group (-COOH) at a 2:1:4 ratio respectively.[60] Oxidation also significantly increases the nanotubes reactivity as well as their wetting properties.

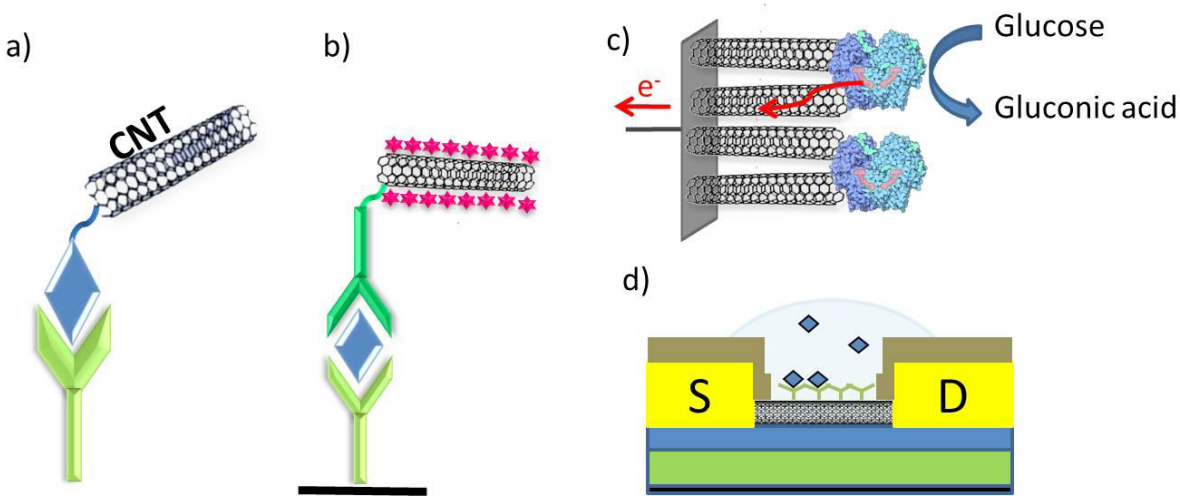

Figure 1.6: Overview of the different SWNT-based biosensor strategies. a) CNT used as a label, b) SWNT used a support for loading tags, c) electrochemical SWNT sensor and d) SWNT-FET sensor. Adapted from ref 61.

The chemical and physical properties of SWNTs make them well suited for sensing applications. SWNTs maintain a high conductivity along their length, which indicates that they are ideal nanoscale electrode materials and nanoscale FETs[62-64]. A good number of literature reviews also suggests that carbon nanotubes have highly sensitive multiplexed

optical properties such as characteristic Raman signal[65] and can be exploited to make entirely nanoscale biosensors that could be used inside cells, or dispersed through a system in order to capture the small amount of analyte present in a system (**figure 1.6 a**).[66] In addition, CNTs act as a support to carry a payload of labels (**figure 1.6 b**),[67] or be used as supports functioning as label-free electrical detectors.[68] Other uses of CNTs in biosensors include CNTs in electrochemical enzyme biosensors that are directly plugged into individual redox enzymes for better transduction.[69] The changes in electrical current due to electrochemical reactions are efficiently transferred through the nanotubes to the metal surface, which are easily detected using voltammetry or amperometry (**figure 1.6 c)**.[70] Last and most important in our case, are FET biosensors based on SWNTs for the detection of single-molecule events. In SWNT-FET based sensors (**figure 1.6 d**), individual nanotubes or their networks are used a channel that provides high-sensitivity for this kind of single molecule detection.[71] FETs that are based on a network of nanotubes are known to offer better reproducibility and manufacturability, however, they show lower sensitivity compared to FETs based on a single SWNT. The first FET sensor that exploited a SWNT demonstrated the detection of gases,[72] followed by the detection of chemical species in liquids using CNT-FET platforms and then finally the sensing of biological molecules, such as metabolites, proteins and nucleic acids using catalytic and affinity based CNT-FETs[73-75.] The sensors reported a good sensitivity however their fabrication could not be up scaled.

The reproducibility involved with the fabrication of SWNTs is still a major drawback. As previously mentioned, SWNTs that are CVD grown present random chiralities. The randomness is the reason why there is a reproducibility issue. The SWNT does not only bridge an electrode gap during growth, but with a successful growth there is no guarantee of the properties that SWNT will display. When it comes to solution based techniques for the fabrication of SWNT based devices, the nanotubes are coated with surfactants and subsequently sonicated for dispersion. This technique generally hinders the electrical properties of the SWNTs because of mechanical cleavage under sonication.[76] Coating the SWNTs with additional materials decreases the sensitivity of the tubes, as they are no longer directly exposed to the environment. Thus, the main setbacks for SWNT based biosensors is the inability to control the properties of as grown SWNTs in addition to the possible damaging and contamination during solution based fabrications. In this thesis, a scalable route to fabricate CNT-based sensors is presented. The fabrication process is performed in a way where the high sensitivity and selectivity of the SWNTs are manageable.

1.3. SWNT Biosensor Theoretical Background

From the first SWNT based biosensor reported back in 1998 by the Dekker group from Delft University[77] and by Avouris from IBM,[78] there has been significant progress made towards characterizing SWNTs as well as integrating SWNTs into working devices. Numerous research groups worldwide have been engaged in using SWNT transistor type devise in hopes to sense a variety of chemical and biological species in a proof-of-concept matter. Many of these projects have demonstrated exceptional results, however there are still a few underlying issues that must be studied and explained through certain experimentation. For instance, the mechanisms governing electrostatic interactions between SWNTs, biological species and device electrodes have not been completely understood. The lack of these conclusions is the underlying reason for disagreement between the numerous research groups till this date.[21,79,80] The study of the properties governing these sensing mechanisms have also been an on going investigation in our work. Regulation agencies such as Health Canada and the Food and Drug Administration require exhaustive research and characterization of health monitoring devices.[21] Hence, to approach commercialization for SWNT based sensing devices for health purposes, such as the detection of bacteria, there must be a thorough understanding of the mechanisms governing the detection of biomolecule capture events. With this, experimental data can be reproduced consistently and regulation agency requirements can be met.

Besides electrostatic interaction, theories have also been proposed to explain why increased sensitivities have been observed for small dimensional sensors.[81] Literature shows that theoretically there is a 5-10 times increase in sensor sensitivity because of the small dimensional electrostatic properties of the transducer element. Except, experimentation has proven that switching the transducer from planar structures to one-dimensional structures such as SWNTs, have increased from μM to femtomolar (fM) levels of detection in some cases. To explain the theory of such a large increase in sensitivity for small dimensional sensors, the kinetics of diffusion has been believed to play a big role.[81] The theory of kinetics of diffusion still requires further work in order to understand the kinetics response of nanomaterial based biosensors.

1.3.1. Proposed Sensing Mechanism

SWNT based transistors as mentioned have a phenomenal potential for electrical detection of biomolecules in solution. The mechanism in charge for sensing purposes however still remains controversial, which obstructs full exploitation of these promising

nanosensors. So far, there have been five theorized sensing mechanisms, which all involve electrostatic interactions between the receptor and analyte, which results in an effect felt by the SWNTs. These mechanisms are chemical doping, electrostatic gating, capacitive coupling, carrier mobility changes, and Schottky barrier (SB) modulation.[82] All of the mentioned sensing mechanisms involve examining the electrochemical interactions between the target analyte and anchored receptor molecules. Each mechanism has its own affect on the SWNT's electrical properties and in order to fully understand this concept; a detailed description of each of the sensing mechanisms would be required. **Figure 1.7** shows a simulation of the effects of the types of sensing mechanisms have on both the characteristic I_{DS} vs. V_g curve as well as the electronic band structure of SWNT based biosensors.

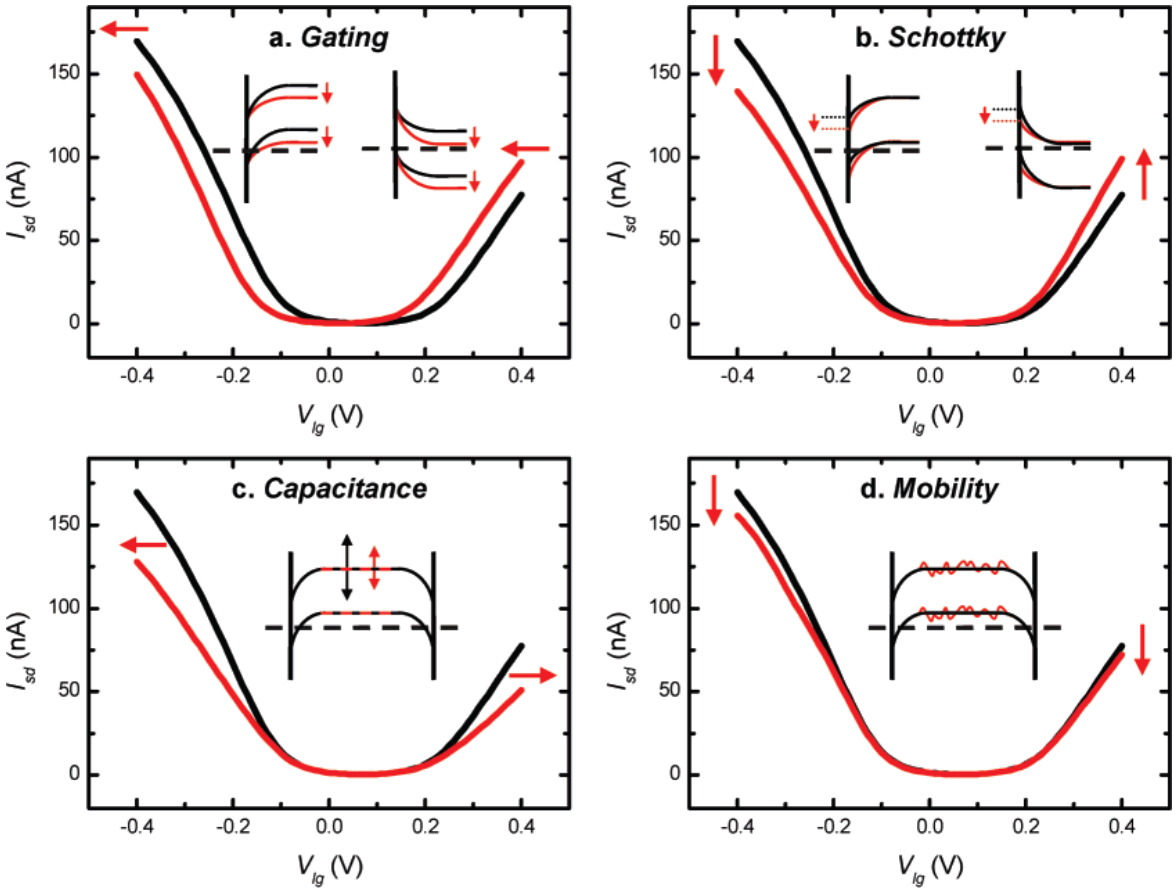

Figure 1.7: Calculated I_d-V_{lg} curves (black) and after (red) protein adsorption of the different sensing mechanisms a) Electrostatic gating/chemical doping, b) Schottky barrier modulation, c) Capacitance Coupling, and d) Mobility Carrier Changes. Adapted from Ref 82.

Figure 1.7 clearly demonstrates that there are subtle differences in the way each sensing mechanism behaves when a change on the surface occurs, affecting the SWNTs

electrical properties. This study provides intake on how the interactions affect both the characteristic I_d-V_g curve as well as the electronic band structure of SWNT devices. The study also provides an insight on how to isolate the different kinds of sensing mechanisms in order to study them individually and in what cases to utilize them. Based off of this study as well as previous experimental and theoretical study completed on the mechanisms governing SWNTs, a paper written by professor Tangs group, electrostatic gating/ chemical doping is the sensing mechanism that will be of main focus. To better understand this sensing mechanism and why it is the mechanism of choice, a detailed understanding is required.

1.3.1.1. Electrostatic Gating

Electrostatic gating is a very important theory that occurs because all biomolecules are capable of carrying a net charge. This net charge depends on two things, 1) the primary structure (amino acid sequence, nucleotides, etc.) and 2) solution conditions (pH, ion type, ion concentration, etc.).[83] When charged specie adsorbs onto the surface of the CNT, the biomolecule will produce an electrostatic gating effect on the CNT molecule.[13] The adsorbed molecules act to tune the surface potential of the CNT, which results in the Fermi level within the channel being increased or decreased depending on the number of biomolecules adsorbed and their charge.[13] The sensing mechanism therefore effectively shifts the threshold voltage of the device, but does not change the current of the device, seen in **figure 1.7a)**.

An important factor that must be considered for this theory is the ionic strength within the electrolyte or buffer. This is due to ionic strength of the solution surrounding the transducing material, which has a large affect on the solution's Debye length and in turn the materials sensing capabilities.[13] The Debye length is refers to a measure the distance the interface into the surrounding solution a surface can experience electrostatic changes.[84] This is due to double layer of charged ions that build up on the surface, and any electrostatic effects that take place any distance further than the Debye length, are screened out. **Equation 2** shows the formula used to calculate the Debye length in solution:

$$\delta = \sqrt{\frac{\varepsilon_o \varepsilon_\tau \kappa_B T}{2 N_A e^2 I}} \qquad \text{Equation 2}$$

Where δ is the Debye length, ε_o is the relative permittivity of the solution, ε_r is the permittivity in a vacuum, K_B is Boltzmann's constant, T is the temperature (in Kelvin), N_A is

Avogadro's Number, e is the elementary charge and I is the ionic strength of the solution. From this equation, it is clear that the ionic strength of the solution is inversely proportional to the Debye's length within the solution. Therefore, as the electrolyte solution gets better at screening out electrostatic effects when there are more ions present within the solution. Hence, for this kind of sensing mechanism, it is important to have low ionic strengths of the solution carrying the target analyte.[13] If this is controlled, the Debye length on the order of the size of the receptor biomolecule will allow for the transducing element to feel the effect of electrostatic changes by the analyte-receptor interfaces.[84]

1.3.1.2. Chemical Doping

SWNTs can be doped, or intercalated, with an electron acceptor or donor. The resulting materials have shown many of the same features such as enhanced electrical conductivity, conduction paramagnetism, and partial or complete reversibility.[85] Chemical doping is an electrical detection mechanism, which involves the direct transfer of charges species to and from a SWNT. Chemical doping as sensing mechanism is responsible for the SWNTs electrical response to gases and liquids. Any species that is in direct contact to the SWNT and is then absorbed on the surface of the SWNT, and is capable of donating or taking away some quantity of an electron to tune the overall conductance of the nanotube is considered as chemical doping.[86] Study shows that rather than the conductance of the SWNT being affected by the overall charge of the dopant molecule, the redox state of the molecule is what actually commands the direction of conductance change.[87] **Figure 1.7** represents the effects of an electron donor on a semiconducting p-type SWNT. The threshold voltage shifts to the negative side as the hole population decreases.

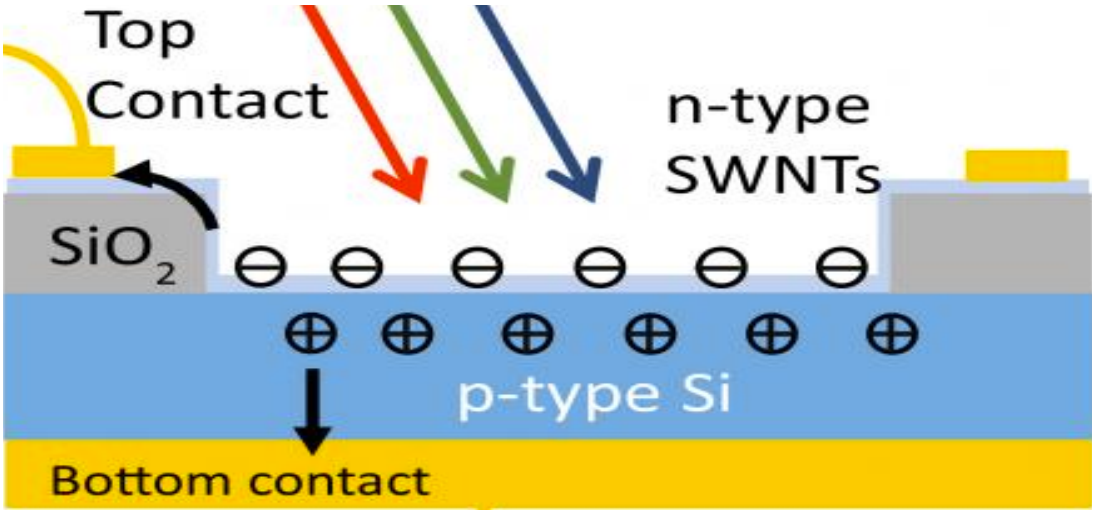

Figure 1.8: Schematic representation of the chemical doping of p-type and n-type SWNTs. Chemical doping is a chemical process that optimizes the properties of SWNTs. [88]

The theoretical study and experimental study of the two sensing mechanisms (electrostatic gating and chemical doping) considered smaller biomolecules such as proteins and nucleic acids as target analytes. However, when studying larger molecules such as bacteria, there are a few differences in the properties that need to be kept in mind. The first difference is the size variance between small molecules (i.e. DNA, proteins, etc.) and bacteria. It is known that the diffusion coefficient is inversely proportional to the molecular weight of the molecule; larger species such as bacteria have smaller diffusion coefficents.[89] This property will therefore result in a decrease in the diffusion capacitance of a 1D system. Although this is not expected to alter the device's sensitivity as bacteria in theory would be able to have multiple capture events, the sensor would however result in an increase in signal. With these theories and experimental observations in mind, the next chapter will discuss the synthesis of SWNT based biosensors that were used for the detection of bacteria.

Chapter 2: Synthesis of PET Based SWNTTF Biosensors

This chapter summarizes the work done on the fabrication of PET based SWNTTF sensors. The growth of SWNTs and their incorporation into the gold plated PET strips will be shown as well as the characterization of the sensors both wet state and dry state will be presented. The rationale of this work was to incorporate these SWNT films into the PET strips to not only enhance the electrical properties of the sensors, but to potentially demonstrate the viability of such nanotubes as a platform technology allowing response to external changes on the surface. Such a phenomena will be useful in the context of bacteria sensor development; opening up the great possibility for real-time, point-of-care, portable SWNT based biosensors.

Some literature review regarding the common fabrication process and surface modification process of the SWNT will be provided, along with a summary of the principles surrounding the characterization techniques typically used for SWNT biosensors.

2.1. Escherichia coli Biosensor

Escherichia coli, most commonly known as *E. coli,* refers to a large group of bacteria that is generally found in the intestines of humans and animals, typically through consumption of contaminated food or water.[90] Most strains of *E. coli* are harmless; however, some strains such as *E. coli* O157: H7, can make people severely sick, causing severe stomach cramps, diarrhea and vomiting. Serious complications of an *E. coli* O157: H7 infection can include kidney failure. *E. coli* infections are generally caused by eating contaminated food or drinking contaminated water and symptoms of an *E. coli* infection usually don't start within about 3 to 4 days after exposure, where the incubation period can last anywhere from 1 day to 10 days.[92] Infections from this bacteria are likely to be more fatal among young children and the elderly. About 5 to 10 percent of those sick develop hemolytic uremic syndrome (HUS), an unusual type of kidney failure and blood disorder, which can be fatal. Some people can have strokes; some may need blood transfusions and kidney dialysis. A diagnosis of *E. coli* infection can only be confirmed through laboratory testing, a process that can take hours to weeks depending on source availability, which is a crucial time for those affected by the bacteria.

For countries like Canada and the United States where there is access to clean water everywhere, it was still reported that an estimated 73,000 illnesses and 2,100 hospitalizations occur annually in the United States because of *E. coli* contamination and an estimated 4000 hospitalizations and 105 deaths associated with 30 known pathogens in

Canada with *E. coli* being 76% of those numbers.[92] The public Health Agency of Canada estimates that 4 million episodes of foodborne and waterborne illness occur each year, and due to the lack of monitoring of this bacteria, the illnesses that arise from it are often misdiagnosed. This leads to expensive and invasive diagnostic procedures, prolonged hospitalization stays, and long term follow-up. In other cases around the world such as South-East Asia where access to clean water and clean food is difficult, 1 in 10 people fall ill every year from diarrheal diseases, estimating that 550 million people are ill and 230 000 of those are deaths.[93]

Detection and monitoring of water or food borne pathogens are of utmost importance to the health and wellbeing of the general public. There exists a plethora of industries as well as individuals that will greatly benefit if disposable devices capable of real-time, sensitive, and selective detection of water- and foodborne pathogens are available to them. With the ability to determine whether current or potential sources of water are contaminated, individuals in developing countries can avoid ingesting diarrhea-causing bacteria such as *E. coli*.

Previous studies in our lab have successfully shown that electrical biosensors using SWNTTFs are able to selectively detect whole M13 bacteriophage coupled with anti-plll M13 antibodies at a 1pM concentration.[41] M13 bacteriophage is a filamentous virus that infects particular strains of *E. coli*. The M13 virus consists of a single stranded of DNA that is enclosed in a 1μM long tube array of 2700 coat proteins.[41] Similarly, but superior, *E. coli* is a rod-shaped bacterium that measures approximately 0.5μM in width by 2μM in length. As previously mentioned regarding the relationship between the diffusion coefficient and molecular weight of the molecule, if the smaller and lighter M13 bacteriophage is detectable at 1pM concentration, then *E. coli* should also be detectable at an even smaller concentration due to its larger size. Hence, the rod-like structure and size of the bacteria as well as the popularity of the bacteria and proof-of-concept work previously done in this lab, made *E. coli* an attractive candidate for a systematic study of SWNT chemiresistive biosensors.

Biosensors have been developed for many different analytes, which range in size from individual ions and small molecules to nucleic acids and proteins up to whole viruses and bacteria. For bacterial sensing, two classes of biosensors have been developed: 1) those that require sample processing to achieve bacterial disruption or lysis in order to liberate the target bacterial component and 2) processing free systems that target whole bacteria. For class 1, biosensors detect bacterial components such as DNA, RNA, enzymes, and secreted exotoxins.[94] The major disadvantage of these systems is the requirement for sample

processing and extra equipment such as reagents, which increases the over all test time and cost. Hence, biosensors that can directly detect whole bacteria without reagents or sample prep, are much more desirable for rapid, cost-effective, point of care testing. This is especially useful because the infectious dose of bacteria for many human pathogens is very low; for E. *coli* O157:H7 it has been reported to be as low as only 10 cells per gram of food or environmental sample.[94]

Significant research efforts have focused upon the detection of whole bacteria. In terms of whole bacteria detection, it has been observed that impedimetric and optical methods are most commonly used. For this work, the impedimetric method for electrochemical biosensors is used because of ease of use, low cost, and point-of-care testing. The impedimetric method will be further discussed in the sensing strategy below.

2.2. Functionalization of SWNT Biosensors

Almost all of the possible applications of carbon nanomaterials such as sensors require a surface modification in order to improve stability, sensitivity, electrical and optical properties, selectivity and biocompatibility depending on the analyte, receptor and transducer. The functionalization of SWNTs is important for rendering them selective to specific analyte molecules. By attaching the receptor molecule to the surface of a biosensor, the SWNTs biosensor becomes selective to specific analyte molecules. These receptors can be attached to the surface via covalent or non-covalent binding. Surface modification in biosensors is specifically used so that there is a decrease in non-specific binding of the various molecules to the transducing component.[95] In this work, antibody Anti-E.*coli* LPS specific for E.*coli* K12 MG1655 is immobilized to the surface. Triton X-100 is dispersed onto the SWNT's for protection of the SWNT's surface against non-specific binding of analyte to receptor molecules.

Due to the very high importance of SWNT functionalization for biosensing applications, possible modification routes are of more importance than others. As stated above, the degree of functionalization of the different carbon nanomaterials and their surface area locations varies significantly. For instance, the edges and defect sites of SWNTs are generally more reactive than other sites. Nanotubes that have a smaller diameter are chemically more reactive due to their increased curvature, with the most reactive sites usually occurring at the most geometrically strained regions.[96,97] In addition to SWNT surface modification, and SWNT film density optimization that has been studied and mentioned above, film geometry

is also a design consideration that can be used to further optimize reproducibility and sensitivity for SWNT containing devices.

Research must progress towards studying the underlying mechanisms of electrical sensing as well as the characterization of the interactions between analyte, receptor and transducer for bacteria; in order to initiate commercialization of SWNT based biosensors from proof-of-concept. Direct comparison of SWNTs in pH controlled environments prior to bacteria detection will assist in understanding the sensing mechanisms at play. This understanding will allow for reproducible and reliable bacteria detection and quantification.

2.3. Fabrication and Method of SWNT-based sensors

2.3.1 Prototype Design and Fabrication

SWNTs have shown to be promising for many fields of use. A lot of possible applications have arisen including electrical sensing, which requires the integration of SWNTs into an electronic circuit. Biosensors can offer a rapid and cost-effective method for bacterial detection, which can be performed at the point of care without the need for a specialist user. The aim of this project was to fabricate a disposable chemiresistive SWNT biosensor that is capable of detecting single whole cell bacteria at the point of care.

The ideal parameters for whole bacteria sensors are almost identical to the necessities for a non-specific biosensor. Depending on where the sensor is being used, such as, stand-alone personal use at home, regular use in a laboratory, or remote regular use off site such was wastewater treatment, the key properties for a commercial biosensor to detect bacteria are the same. Ultimately, they should be inexpensive, small, easy to operate with little to no sample preparation and be label free. Some key requirements for an ideal biosensor shown in **Table 2.1** are included in the prototype design of this project.

Parameter	Value or Quality
Sensitivity	Less than 10^3 CFU/mL
Specificity	Can distinguish different serotypes of bacteria (e.g., can distinguish *E. coli* Nissle 1917 from *E. coli* O157:H7), minimal background, must operate in complex matrices (e.g., clinical samples such as sputum and blood, food, and beverage samples)
Speed	5-10 min for a single test
Size	Compact, portable device that can operate at the site of interest
Sample Processing	Label free with minimal sample processing
Stability	Biorecognition element must be stable at the high temperatures experienced in some countries (e.g., up to 45°C) for several months to allow for good shelf life
Skill of Operator	No specialist training needed to use the assay, can be used by patients

Table 2.1: Requirements for an ideal bacterial sensor. Copyright from reference 94.

To achieve a realistic disposable sensor that fits the requirements listed in **Table 2.1**, the first step is for a cost-efficient disposable substrate. By customizing a premade substrate that is typically used for blood glucose sensors, a cost effective proof of concept device is fabricated. **Figure 2.1** shows a fully fabricated substrate prior to SWNT transfer. Once the transfer is completed, the substrate is referred to as a SWNT based electrical biosensor. All information pertaining to the synthesis of SWNTs, substrate fabrication, device cleaning, and transferring can be in *appendix A.*

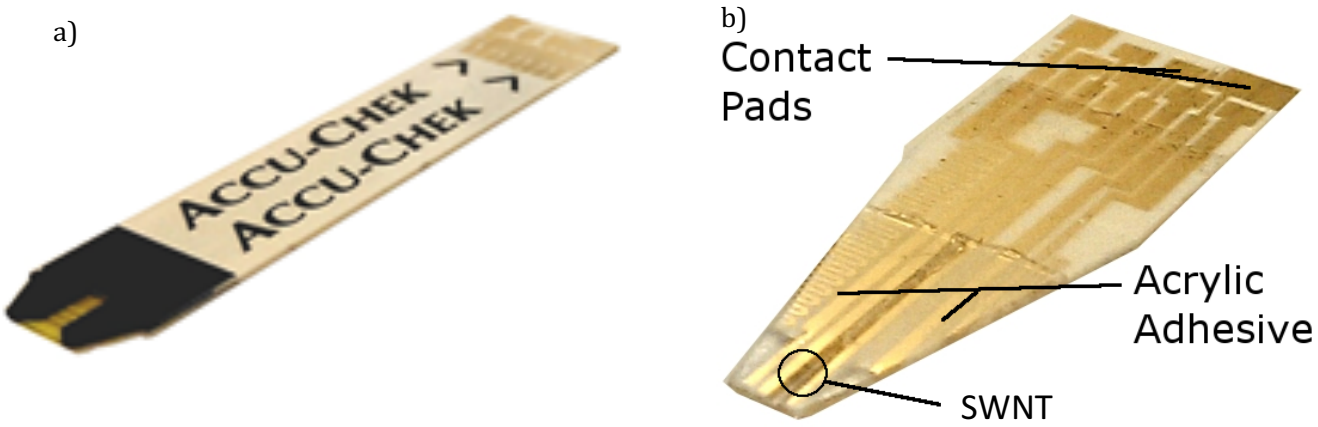

Figure 2.1: a) Premade substrate used for blood glucose sensors stripped and refabricated to a SWNT electrical biosensor shown in b). Note the location of where the SWNT film will be transferred

The sensor shown in **Figure 2.1** indicates how simple it is to fabricate a SWNT bacteria-testing strip. By simply removing the accu-check cover and adhesives on the surface, cutting the strip into the shape desired, and transferring a SWNT on to the desired location, a cost-effect, disposable sensor is invented. There are a few features that are important on a substrate in order for a successful fabrication. These are the pre-patterned gold electrodes, the contact pads for the connector, the adhesive layer and the location surface area for the SWNT. By removing the accu-check cover and acrylic adhesives on the strip, these strips are used as substrates for SWNT chemiresistors. SWNTs are transferred onto the aforementioned surface area on the substrates without the use of any reagents or prep to the surface. The SWNTs can be directly transferred from the silicon substrates to the disposable blood glucose substrate. This simple transfer indicates the simplicity behind the fabrication of these SWNT biosensors. All information pertaining the removal of adhesives, cleaning, and SWNT growth/transfer can be found in detail in *appendix a.*

After the bare transfer of SWNTs to the test strip, an acrylic adhesive is used to coat the gold electrodes so that only the SWNT is exposed to the various testing solutions. This controlled exposure allows for a better understanding of the interactions between the gold electrodes and the nanotubes, and the nanotubes to the solutions. Specifically, interactions between the gold electrodes to SWNTs and gold electrodes to the testing solutions can be ruled out as a cause for unwanted electrical responses.

It is important to note that the prototype design involved a number of iterations as well as trial and error in order to obtain a reliable electrical connection to the substrate. Without a reliable stable connection, the electrical sensor did not allow for stability and reproducibility.

In order to run an electrochemical test on the fabricated SWNT electric biosensor, and to ensure proper stability and reproducibility, a suitable connector was designed specifically for the SWNT test strip. **Figure 2.2** is an image of the connector that was built with appropriate dimensions for proper connection and circuit flow. This connector was specific for a SWNT test strip that used contact pads 3 and 4. Once the SWNT test strip was directly inserted into the connector, dry state characterization was completed for each of the devices.

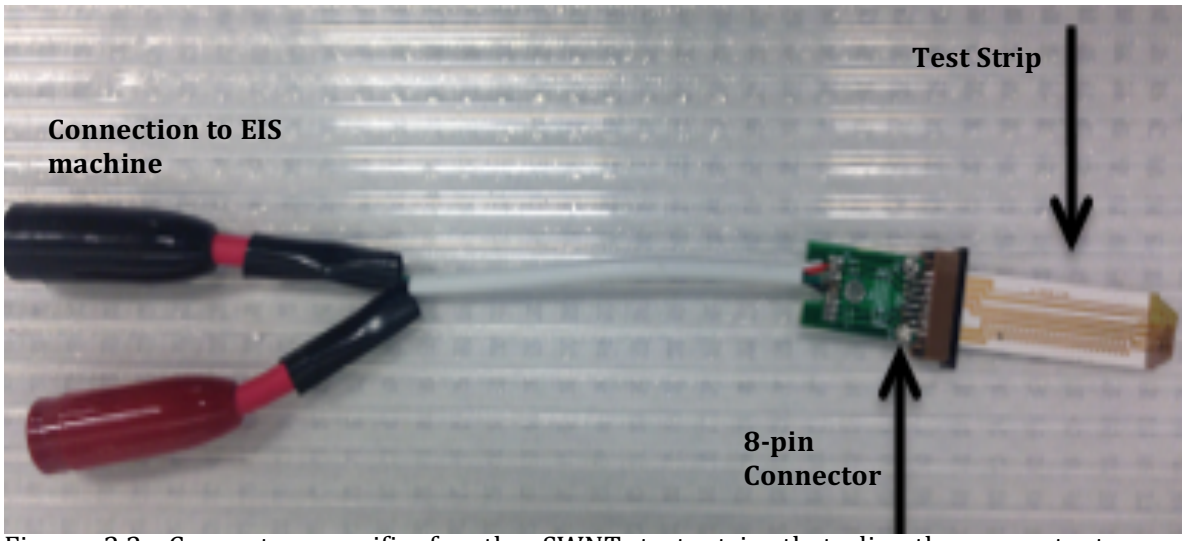

Figure 2.2: Connector specific for the SWNT test strip that directly connects to an Electrochemical spectroscopy machine.

2.3.2 Dry State Characterization

Dry state characterization for all steps from SWNT growth and transfer to device fabrication is vital and must be concluded throughout the fabrication process. The simplest method for material characterization, such as determining whether or not SWNT synthesis is successful prior to SWNT transfer is Raman Spectroscopy. A Raman peak analysis is accomplished after transfer and patterning to ensure that there has been no damage to any of the SWNT films during the fabrication process. Raman spectroscopy is used throughout the period of this work using the Horiba (Jobin Yvon) HR800 Raman spectrometer.

Imaging techniques such as atomic force microscopy (AFM) and scanning electron microscopy (SEM) are used to determine the SWNTs film density after growth. AFM can also be used prior to SWNT growth to confirm a proper distribution of catalyst particles on the substrate. As mentioned, the aim of this work was to use low-density SWNT films because of its enhanced sensitivity to biomolecules. For this reason, characterizing via images of the films is crucial. Prior to any device fabrication, the successful synthesis of SWNTs is the most

important part of the project. The reproducibility of the synthesis of low density SWNTs was the first goal of this project. In addition to ensuring the reproducibility and success of low dense films, imaging techniques are also used to determine proper device patterning and cleaning during fabrication. Atomic force microscopy also has the ability to provide nanotube parameters such as tube diameter and tube junction height prior to biomolecule detection. This information allows us for a better understanding of the SWNT surface area for bacteria detection. All AFM imaging was completed using Digital Instruments Nanoscope Multimode AFM.

Prior to this study, a study was conducted to determine whether or not there was any response to the dry state electrical behavior of SWNTs. This study fabricated devices with a back-gating through a 50nm SiO_2 wafer. Using a gate voltage varying from -5V to 5V the drain current was monitored at a constant drain voltage of 10mV. An on/off ratio (I_{on}/I_{off}) was determined allowing for an overall switching capability of the film. These results were used to compare the device response to biomolecule sensing. Results of this study concluded that based on the dry state electrical characterization of SWNTs, there is a correlation between dry state electrical behavior of SWNTs and their electrical response to biomolecules. This conclusion allows for this project to move forward with biomolecule detection on the surface of these SWNT films. The dry state resistance of each device is measured as well as the surface area of the film being exposed to any testing solutions. All electrical measurements were performed using either an Electrochemical Impedance Spectroscopy or a CH400E series Electrochemical Analyzer.

2.3.3 Sensing Strategy

Once the dry state characterization of the SWNTs and the testing strips are confirmed, the sensing strategy that is used throughout this project is impedance spectroscopy. Since the 19th century, after Oliver Heaviside created the term "impedance," electrochemical impedance spectroscopy (EIS) has been employed to characterize different biological systems.[98] Electrical detection methods such as impedance spectroscopy is a much simpler instrumentation method compared to those such as optical methods, that ensures lower cost and power consumption. Electrical methods were chosen for this project because these methods are ideally suitable for implementation of label-free detection approaches, giving a number of advantages for the biomedical assay. Some important advantages include elimination of sample modification, avoiding the influence of labels on the binding property, and above all the possibility of real-time monitoring of binding interactions. Field-effect

transistors (FET) are the most common among such biosensors that uses impediametric measurements instead of DC because it offers better signal to noise ratio as well as the possibility of changing an additional important parameter; frequency.

Ideally an FET contains source and drain electrodes, a semiconducting channel and a gate electrode.[99] Applied gate voltage (V_G) modulates electrical transport through the semiconducting channel. The gate will regulate the electric field generated vertical to the surface of the channel. This electric field can be generated through a solid-state dielectric such as silicon oxide, or in a liquid. **Figure 2.3** shows a schematic of a solid-state FET (back-gate- figure 2.3a) and a liquid FET (liquid gate-figure 2.3b).

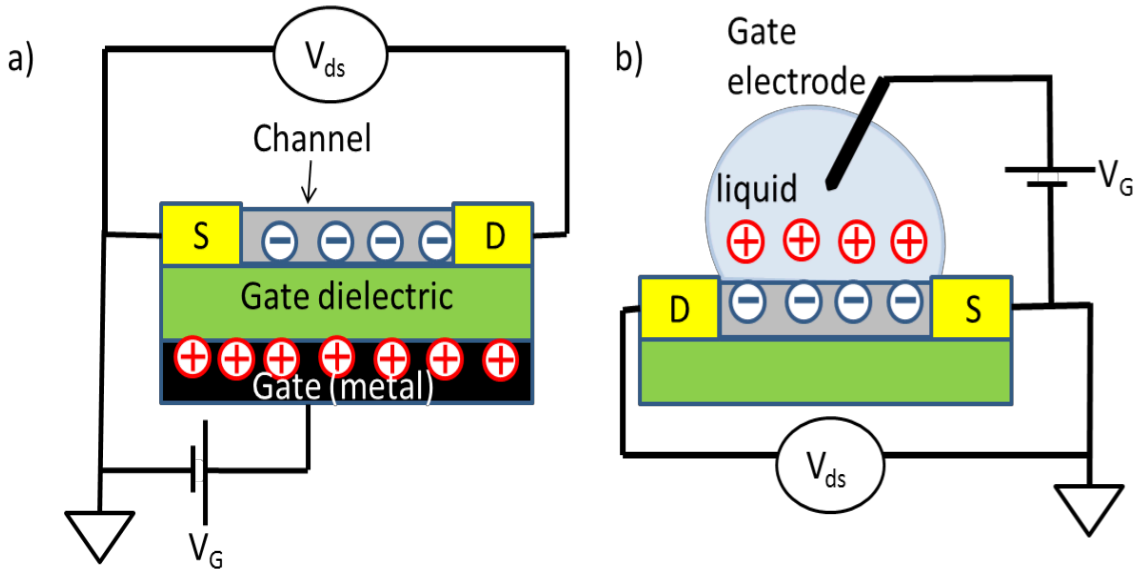

Figure 2.3: Schematic representation of a solid-state FET (a) and a liquid gate FET (b)

Research indicates that a liquid electrochemical gated configuration is much more promising when it comes to medical diagnostics because of its ability to detect analytes directly in biological units. This reduces the possibility of contamination of substances as well as a decrease in risks of illness occurring from sample interactions. In a liquid gate FET, such as the one used for this project, the device is immersed into the liquid containing the biological sample, and the reference electrode is used to apply the gate voltage. The conductivity of the system as a function of the charge-carrier concentration is the basis of the electrochemical-gated device, which is controlled by the electrochemical potential.[100] The gating effect is accomplished through the creation of an electrical double layer (EDL) on the surface of the semiconductor. The change in the potential of the gating electrode leads to a change of the electrostatic potential over the EDL. Therefore, the charges that form the EDL

influences the interfacial potential and thus affecting the source-drain current.[100] With respect to bacteria detection on the surface of the electrode, the adsorption of additional charges due to biorecognition reactions, such as binding of analyte to receptor or bacteria to antibody, the changes on the surface of the semiconductor (SWNT) will lead to changes in transport characteristics of the device. These changes that occur can also be detected by measuring the source-drain current.[101]

The method that is used to detect the changes in the transport characteristics stated above for the FET is impedance measurements. *Impedance* (Z)- is equivalent to resistance for an AC circuit. It describes the voltage to current ratio as well as the phase difference between the two parameters.[102] Electrochemical impedance spectroscopy (EIS) is a standard measurement of the impedance at the surface of a working electrode in electrochemistry. This process involves a small sinusoidal signal, via a potentiostat; at some set direct current (dc) level (V_0) and measuring the resulting current. The input signal is shown by the equation below:

$$V(t)=V_0+|V|\sin(\omega t) \qquad \text{Equation 3}$$

While the measured current is as follows:

$$I(t)=I_0+|I|\sin(\omega t+\varphi) \qquad \text{Equation 4}$$

The most important parameters are the dc level (V_0), which sets a point on an IV (current vs. voltage) curve for the particular electrochemical reaction, the magnitude of the input voltage |V| and the frequency ω ($2\pi f$). The impedance Z (ω) as a function of frequency can be calculated using Ohms Law:

$$Z(\omega) = V(t) / I(t) \qquad \text{Equation 5}$$

Impedance can be defined as the total opposition a device or circuit offers to the flow of a current at a given frequency, and unless the impedance is purely resistive it will be a complex quantity, which can be graphically shown on a vector plane.[103] An impedance vector, calculated in ohms (Ω) consists of a real part (resistance, Z_r) and an imaginary part (reactance Z_j) where the sum of these two parts represents a series connection of resistance and reactance. The complex impedance will be dependent on the frequency of the sinusoidal signal used to make the measurement.[103] Therefore, using EIS, measurements will are made

over a range of frequencies suitable for testing the devices in order to obtain an impedance spectrum. This collected data will contain a great deal of information about the electrode surface of the device. It will be crucial for understanding the mechanism of sensing as well as identifying the parameters best set for obtaining the highest sensitivity and selectivity.

The main reason for using EIS in biosensors is that it provides very accurate measurements of changes to a surface caused by molecular attachments. For EIS biosensing applications there are two main forms of electrodes to be noted. The first is the interdigitated electrode (IDE), which has the ability to measure changes in the in- plane impedance between the two electrodes. This is typically non-Faradaic in nature and will show us changes in the dielectric or conductive properties of the material coating the electrodes.[103] The second electrode is commonly referred to as a functionalized electrode where the impedance between the electrode and the solution will be measured. Selectively attaching analyte molecules to a biosensor coating will change EIS responses. For this project EIS responses will be observed in bare state, followed by the addition of a sensing layer, and finally with an antibody to receptor attachment.

Impedimetric biosensors function by an analyte-bioreceptor interaction causing a change in capacitance and electron transfer resistance across a working electrode surface as shown in **figure 2.4**. Previous studies theoretically show that as the concentration of the analyte increases with respect to higher analyte binding, the impedance across the electrode surface changes and is detected at a transducer. The overall impedance is seen to increase or decrease depending on the analyte used. This electrical method in contrast to other electrochemical detection methods requires no oxidation or reduction process. Hence, even without the use of a mediator the range for possible analyte molecules broadens. Bioreceptors used in these cases are commonly antibodies, which for this project, antibody specific to bacteria are used.

Electrochemical Impedance Spectroscopy has become a progressively attractive technique in many biosensing applications. The simplicity of the technique attracts many researchers towards this concept, however some disadvantages lie within the complexity of the mathematical concept. In general, the aforementioned impedance denoted as *(Z)*, can be correlated directly with analyte binding to a biosensors surface. Z is recorded over a wide range of frequency *(1Hz-1MHz)* with respect to time, where two other major components are measured, such as resistance *(R)* and capacitance *(C)*. Impedance data is often represented as Nyquist plots, which is how the data for this project will be presented, where R or Z_{real} is

termed as the "real component" on the x-axis and C or Z_{img} is termed as the "imaginary component" on the y-axis as shown in **figure 2.4b)**.

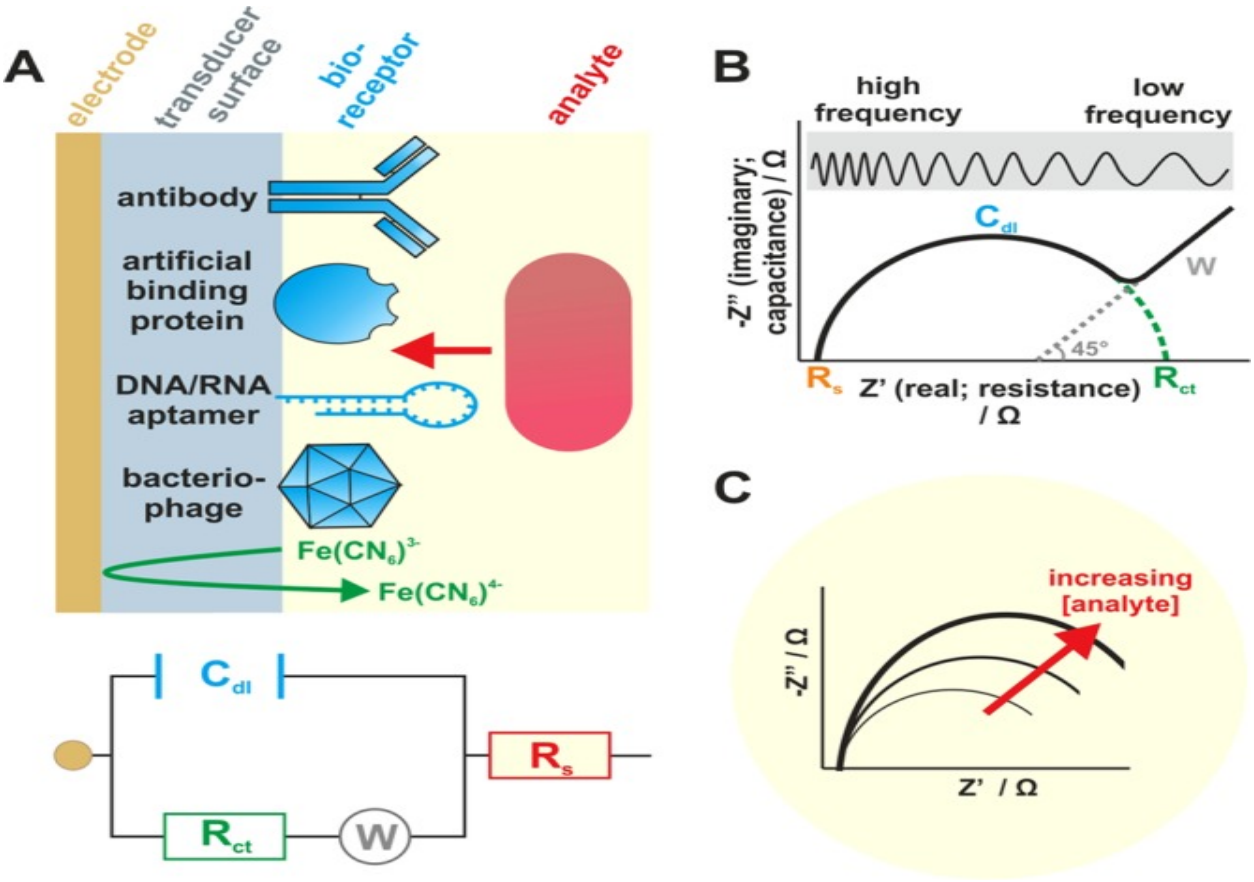

Figure 2.4: A schematic representation of the structure and electrochemical function of impedance-based biosensors for bacterial detection. A) Construction of a sensor, which typically comprises of an electrode surface functionalized of bio-receptors. The Randles circuit illustrates the components of the system where double-layer capacitance *(C_{dl})*, charge transfer resistance *(R_{ct})*, solution resistance *(R_s)*, and Warburg impedance *(W)*, which is usually observed at low frequencies but will not be observed for this projects results. B) is a representation of a Nyquist plot that corresponds to the Randles circuit shown in a). C) An impedance presentation of changes resulting from analyte-surface interactions with respect to increase in analyte concentration. Copyright from Reference 104.

Data analysis for impedimetric detection of analytes is specific to high frequency and low frequency. At high frequencies, the major component of impedance is derived from the resistance of the solution (solution resistance [R_s]), and at low frequencies, impedance is measured from the resistance of the flow of electrons or charge to electrode surface (charge transfer resistance [R_{ct}]. The derived impedance plot can then be translated into an equivalent circuit model proposed by Randles. Changes occurring on the surface of the electrode, either by analyte binding or layer-by-layer construction can be plotted

quantitatively. Results for this project will be shown via Nyquist plots prior to and after fitting of the results.

In order to analyze the results obtained through impedance spectroscopy, a proper model and fitting of the real impedance vs. the imaginary impedance must be conducted. The fitting of the results allows us to mathematically extract the resistance and capacitance from Z_{real} and Z_{img}. Using Matlab, mathematical simulation software, the resistance, capacitance and other required parameters are extracted by generating and modeling a fit that is based on the Randles equivalent circuit. The corresponding mathematical equations will be presented in the results section.

2.4 Results and Discussion

2.4.1 Dry State Characterization

Device characterization is very important throughout all fabrication processes to ensure all protocols are working properly. As mentioned above, the best and easiest way to ensure flawless nanotubes in a SWNT film is to measure the film's Raman spectrum. **Figure 2.5** is a typical representation of what a SWNT growth looks like as they are grown, after transfer and post patterning. This fabrication process is the ideal process for when SiO_2 wafers were used before and after transferring. This data is assumed to be identical for when transferring and patterning SWNT's to the disposable strips.

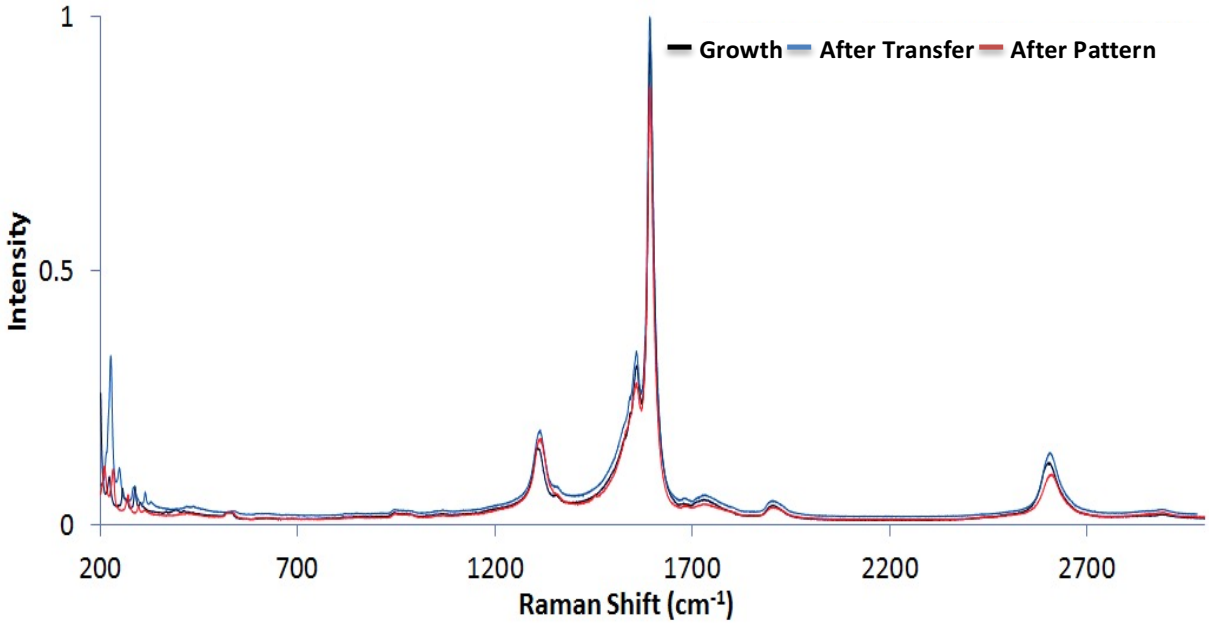

Figure 2.5: A Raman spectra of a SWNT film taken after growth, after transfer and after patterning on a SiO_2 wafer.

The aforementioned synthesis technique of single walled carbon nanotubes results in a random and uncontrolled growth due to the nature of the catalyst deposition process on the wafer. However, the main conclusion that is made after Raman analysis conducted on every growth as shown in **figure 2.5**, is that all the fabrications steps that lead up to a finalized sensing device are successful. As shown, it is clear that all the steps required for a successful SWNT transfer did not cause any damages to the SWNTs. In addition to the unsystematic nature of the catalyst cocktail deposition, there is also no control over the individual radius of the nanotubes as well as electric properties. Statistically, because of randomization of the catalyst cocktail on the substrate, a network of nanotubes present on the substrate after growth tend to be 33% metallic while the other 66% are semiconducting nanotubes.

The Raman spectrum of a SWNT film gives us enough information to conclude that SWNTs are indeed present throughout the film. The location and intensity at peaks 120cm^{-1} to 250cm^{-1} denoted as the radial breathing mode (RBM) range, are subsequently random depending on the spot studied of the SWNT film. All SWNT film samples thus do contain a number of RBM peaks with a strong signal in this range indicating that carbon nanotubes are single walled. Other important peaks that indicate the film is composed of SWNTs are the D, G and 2D bands shown below. As shown in **figure 2.6**, at approximately 1350cm^{-1}, a D band can be seen, followed by a G band at 1600cm^{-1}, and lastly a 2D band a 2700cm^{-1}, respectively. On average, the majority of the samples used contain a very high G:D band ratio instigating that the films do contain pure SWNTs.

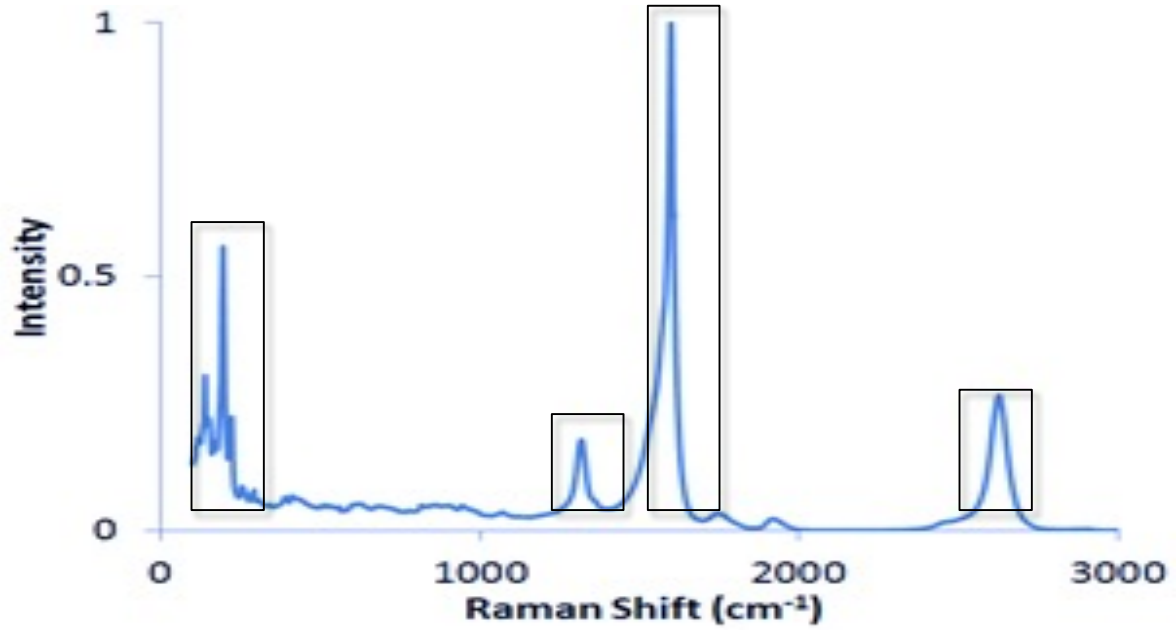

Figure 2.6: A Raman spectrum of a SWNT film growth showing a RBM at 120-250cm^{-1}, a D band at approximately 1350cm^{-1}, a G band at 1600cm^{-1} and lastly a 2D band at 2700cm^{-1}.

Some key things to note based off these results are the fact that after all fabrication processes the SWNT's were not damaged in anyway. They were consistent and present from the growth step to the final device fabrication. The only changes in peak intensities were observed when the laser of the Raman was at a different location on the SWNT film. After determining the successful growth of SWNT's, the transfer and the patterning, the next step was to determine the density of the films. It was observed that the center of the substrate after growth had the highest density of SWNT's compared to the outer parameters of the substrate. AFM images for the analysis of SWNTs can be seen in **figure 2.7** below.

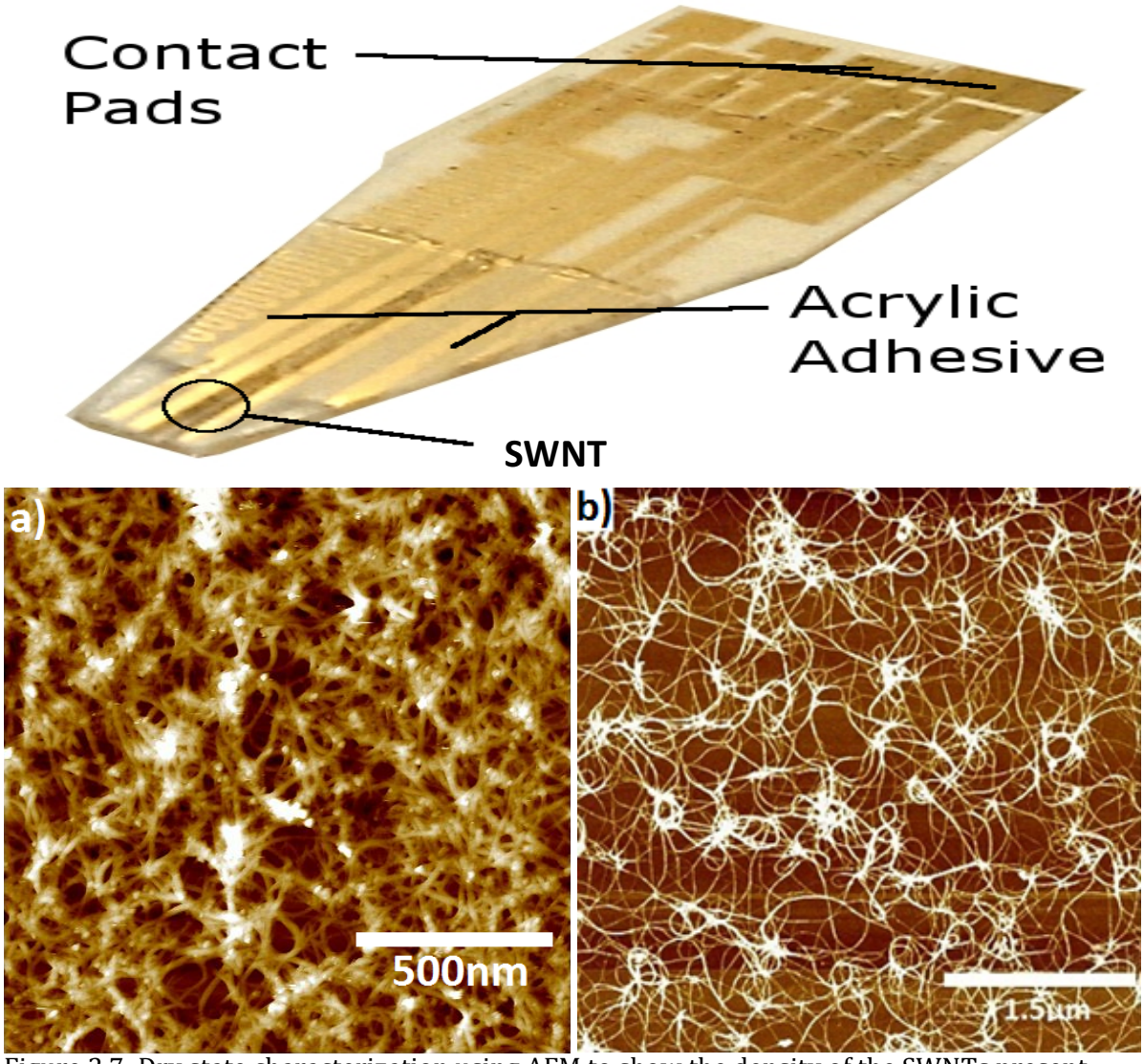

Figure 2.7: Dry state characterization using AFM to show the density of the SWNTs present on the film post growth and transfer. A) Shows a higher density of SWNTs present on the film compared to B) showing a lower density of SWNTs present on the film. The sensor above indicates where the transfer of these SWNTs will be.

Figure 2.7 is a representation of the two types of films that were observed throughout the growth of SWNTs. **Figure 2.7a)** shows a higher tube density than the films present in figure b) indicating that the catalyst used was a typical non-diluted catalyst that was capable of promoting additional SWNT growth. Nanotube bundling is evident in both images, which is a consequence of the random placement of catalyst nanoparticles on the substrate prior to growth via spin coating. The reason behind **figure 2.7b)** is the theory behind recent studies, which demonstrates that the lower density SWNTs are capable of achieving higher sensitivities for biomolecule detection.[105] According to experimental work, lower density

films are more dependent on semiconducting tubes, which in turn are more sensitive to energy shifts at the Fermi level. Based off of these theories and experimental work, the tubes used to fabricate the devices in this project were modeled after these films so that the enhanced sensitivity can be utilized.

AFM measurements are also used to study the individual nanotube diameter. A disadvantage of using the disposable substrate is that the nanotube diameter is not measureable due to the roughness of the surface under the AFM. In order to understand the diameter of the tubes after transfer onto the disposable substrate, the same protocol was conducted but with a silicon substrate. The AFM measurements on the silicon substrate show an average diameter between 1.8nm-3.6nm. The higher end of the radii indicates the probability of having a bundle of nanotubes present on the film. With radii numbers, and similar height profiles with large height variations, as well as stacking and curvature of the tubes indicates that single walled nanotubes are in fact present on the films.

With results from Raman spectrum shown in **figure 2.5** and **figure 2.6** as well as AFM images shown in **figure 2.7**, it has been confirmed that the nanotubes used for the fabrication of our portable device are indeed low-high density SWNT films. After confirmation of the tubes, the next step is to characterize the fabricated devices in wet state using DI water followed by pH sensing.

2.4.2 DI Water Characterization

The first test conducted on each fully fabricated SWNT device is a DI water test. The first purpose of this test was to ensure proper SWNT fabrication had occurred and that the electrochemical response was not from the gold surface below but from the SWNT film. In order to determine that the SWNT is responding, the response from the SWNT device is compared to a bare substrate that is fully fabricated using the same protocol but without the SWNT film. If a shift in overall resistance and capacitance is observed, that indicates that the water surrounding the SWNT alters the electric field and thereby doping the pi network of the SWNT film. **Figure 2.8** shows a nyquist plot of DI water on a bare gold substrate without the use of a SWNT.

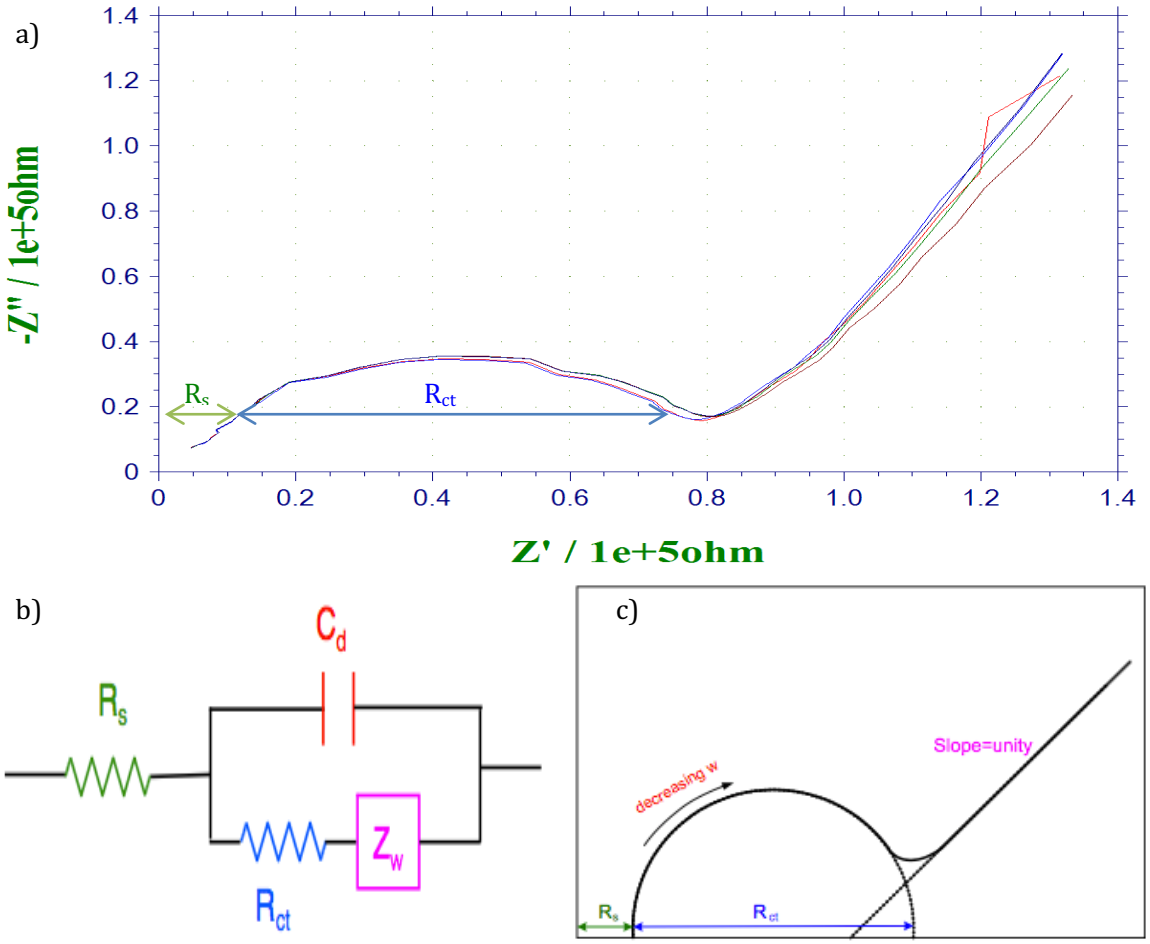

Figure 2.8: A) A nyquist plot for DI Water of a bare gold substrate. The corresponding randles circuit can be seen in b) and figure c) is an ideal nyquist plot arising from the Randles circuit shown in b) indicating where the R_s and R_{ct} components come from.[102]

Figure 2.8 shows a disposable substrate in DI Water before a SWNT film deposition. For impedance measurements on these substrates, a small sinusoidal AC voltage of 5mV is applied, and the current response was determined. The in-phase current response determines the real (resistive) component (x-axis) and the out-of-phase current response determines the imaginary (capacitive) component (y-axis). It is important that the AC probe voltage is small enough so that the system response is linear, allowing simple equivalent circuit analysis. The impedance method in this case is very powerful in the sense that it allows the characterization of physiochemical processes of widely differing time constants, sampling electron transfer at high frequency and mass transfer at low frequency.[102] Impedance results are commonly fitted to equivalent circuits of resistors and capacitors, such as the aforementioned Randles circuit shown in **figure 2.8b)**, which is often used to interpret simple electrochemical systems such as a simple DI water test to determine the basic resistance and capacitance of the overall system. This equivalent circuit yields the Nyquist plot shown in **figure 2.8c)**, which provides a visual insight into the system dynamics. In **figure 2.8c),** which is a schematic representation of the data shown in **figure 2.8a),** the R_{ct} is the charge transfer resistance, which is inversely proportional to the rate of electron transfer. The C_d is the double layer capacitance, and the R_s is the solution resistance. Z_w in this case is the Warburg impedance, which arises from the mass-transfer limitations. The Warburg impedance is only seen at the low frequency range where mass transfer limitations occur, which can be seen for bare gold electrodes, however this is not seen when there is an addition of a SWNT because of the frequency range being much lower. For bare gold electrodes in DI water, the range is limited to 1MHz to 10mHz, however when there is a SWNT deposited to the substrate, the overall frequency range can be is lowered to 1HZ-100KHz. It is important to note from here on out that the solution resistance arises primarily from the electrolyte resistance and is analytically useful mainly in conductivity sensors. The Warburg impedance, which can be used to measure effective diffusion coefficients, is rarely useful for analytical applications and hence will not be discussed here on out.

The overall shift in resistance tends to vary with the addition of a SWNT film indicating that there is a change in sensitivity of the sensor. With a change in sensitivity of the sensor, meaning signal amplification, the possibility of detecting a lower concentration of bacteria becomes possible. Studies have shown that a gold plated electrode for sensing *E. coli* K-12 bacteria has a detection limit of 10^4-10^7 cfu/mL.[104] With the addition of a SWNT, the limit of detection due to the capability of altering SWNTs as desired, such as making them specific

and more sensitive could potentially go down to 10^1-10^2 cfu/mL. **Figure 2.9** shows the basic measurement of DI Water on the same substrate as shown above except with the addition of a SWNT. With the addition of a SWNT to the surface of the sensor, the overall signal become amplified, the biosensor can achieve a lower limit of detection due to their high surface area, we can now have favorable electronic properties and electrocatalytic activity as well as good biocompatibility induced by the nanometer size and specific physiochemical characteristics.

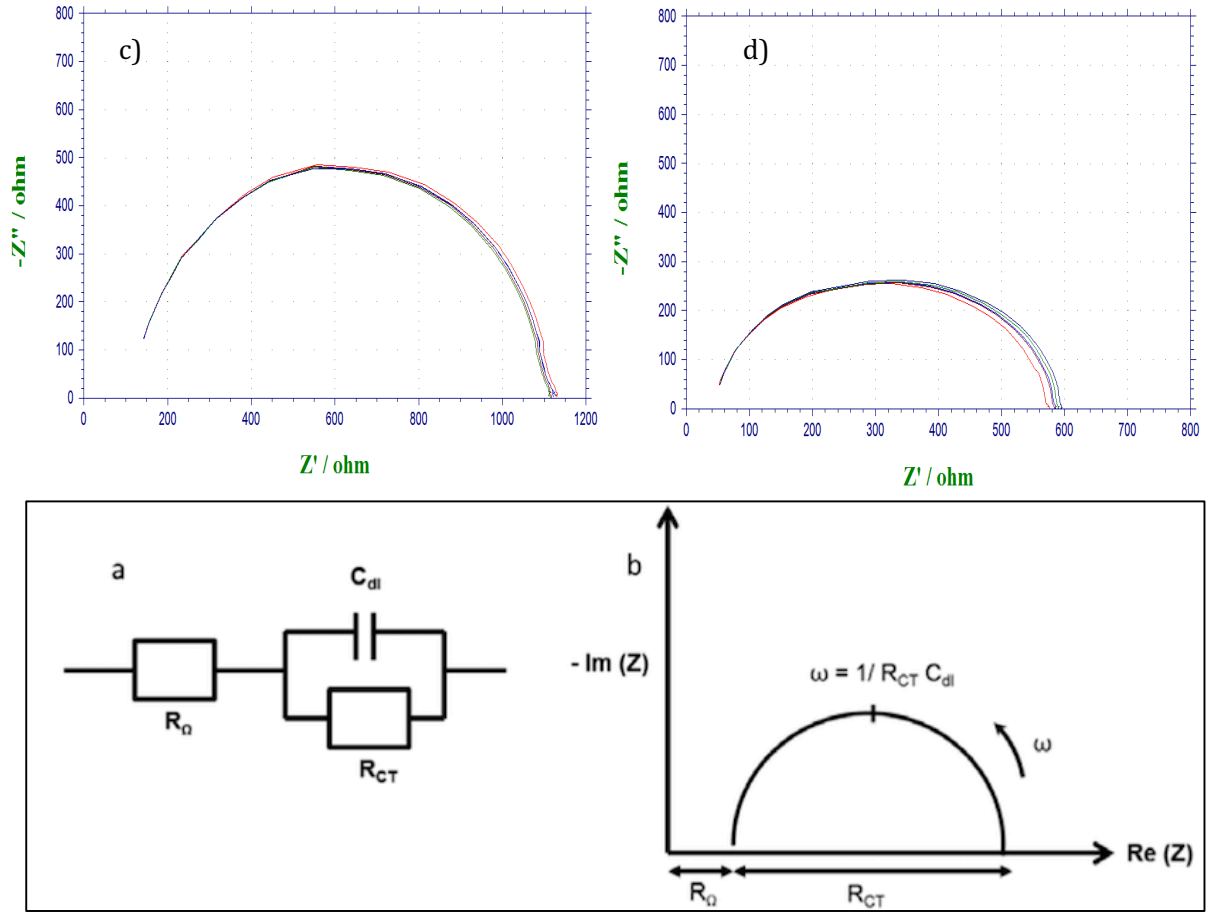

Figure 2.9: Representative SWNT substrate measurements taken during DI Water for a series of 5 trials to show sensor stability in c) Z_{real} vs Z_{img} and d) Z_{real} vs Z_{img}. Figure a) is a schematic representation of the randles electrochemical circuit without the Warburg impedance and b) is the corresponding nyquist plot.

A nyquist plot that is shown in figure 2.9b typically presents the impedance spectrum of the cell suspension in DI water. The equivalent circuit of the biosensor measuring the impedance of the cell suspension in DI water consists of solution resistance between two sets of finger electrodes (R_s), the double layer capacitance (C_{dl}), and electron transfer resistance

(R_{ct}). In this case there is no Warburg impedance because of the addition of the SWNT that has the ability to amplify the signal at high frequencies. The cell suspended in DI water may release some electrochemical active composites to DI Water, which is seen through the Warburg impedance, however this information is neglected because of the material that is provided at high frequency. Recent studies and literature indicates that the impedance response measured at a fixed frequency of 1kHZ as a function of time provides clear enough evidence of ion release from cells that decreases the impedance.[105] Studies also show that the two major regions that indicate major impedance responses to various solution environments such as DI Water to PB buffers and solutions containing bacteria, are the double layer region (from 1Hz to 500Hz) and the resistive region (from 500Hz to 100kHz). For these reasons as seen in data presented in **figure 2.9 c) and d),** fitting for the solution resistance, charge transfer resistance and double layer capacitance is completed and shown below in **figure 2.10.**

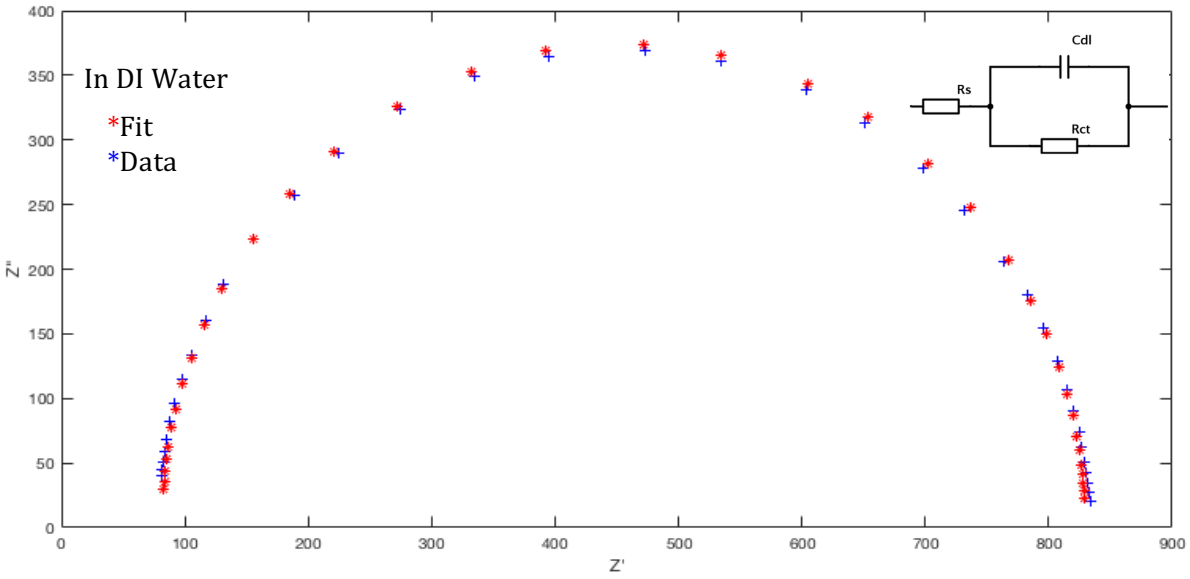

Figure 2.10: Fitted data for SWNT biosensor in DI Water using the Randles circuit shown in the top corner.

When the data from the measured impedance spectra were input into the aforementioned equivalent circuit, the fitting spectra shown in blue is obtained, which matches very well with their respected measured spectra. This indicates that the equivalent circuit provides a feasible model to represent the behavior of the SWNT biosensor in DI water. The calculated R_s of the data presented in **figure 2.10** is 81.52 Ω, the R_{ct} is calculated to be 748.3 Ω, and the

C_{dl} has a value of 5.488e-08μf. The equations used to calculate the fit based on the Randles circuit involving resistors and capacitors is shown below:

$$Z_{resistor} = R \qquad \text{Equation 6}$$

$$Z_{capacitor} = -j\frac{1}{\omega C} = \frac{1}{j\omega C} \qquad \text{Equation 7}$$

For every resistance and capacitance present in the Randles circuit, the equations above are used. For example for total resistance:

$$Z_{total} = Z_{R_s} + Z_{R_{ct}} \qquad \text{Equation 8}$$

Electrical conductivity is the measure of a materials ability to allow the transport of an electric charge represented by units S/m (siemens per meter). For a given electric field in a material, a higher conductivity material will produce more current flow than a low conductivity material. Conductivity is analogous to the inverse of resistance. Electrical conductivity, which is reciprocal to electrical resistivity, an object of uniform cross section has a resistance proportional to its resistivity and length and inversely proportional to its cross-sectional area. With respect to water, conductivity is a measure of water's capability to pass electrical flow. This ability is directly related to the concentration of ions present in water. These conductive ions come from dissolved salts and inorganic materials such as alkalis, chlorides, sulfides and carbonate compounds. Deionized water is a poor electrical conductor, having a resistivity of 18.2 megohm and a conductivity of 0.055 μS.[106] Milli-Q water that has been purified using an ion exchange cartridge, has a value much greater than 18.2 MΩ.[106] Due to the relationship between conductivity and resistance, the lower the conductivity the higher the resistance and the overall change conductivity has on the absolute impedance, the conductivity of the samples must be kept constant. **Figure 2.11** shows the difference between the impedance of DI water and Milli Q water. It can be seen that the Milli Q water has a much greater overall resistance than DI Water (**Table 2.2).**

	R_s	R_{ct}	C_{dl}
Milli-Q Water	218.6	1603	7.655e-08
DI Water	25.83	242.2	9.782e-08

Table 2.2: Resistance and Capacitance of Milli-Q water compared to DI Water

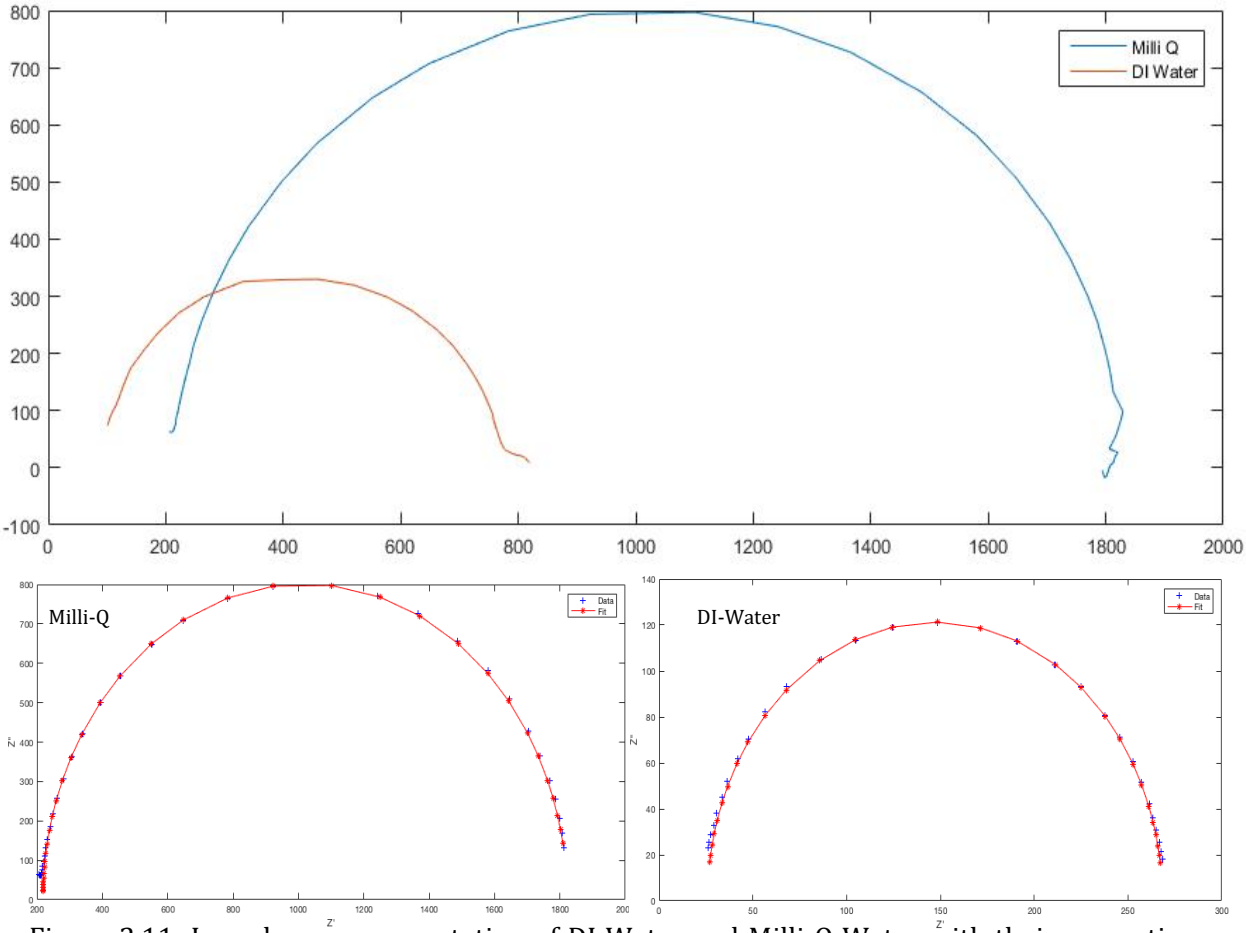

Figure 2.11: Impedance representation of DI Water and Milli-Q Water with their respective fittings.

Milli-Q water has an R_{total} of 1821.6 Ω with a R_s of 218.6 Ω, a R_{ct} of 1603 Ω and a C_{dl} of 7.655e-08 µf. DI Water has an R_{total} of 268.33 Ω, with a R_s of 25.83 Ω, a R_{ct} of 242.5 Ω, and a C_{dl} of 9.782e-08 µf. DI Water was chosen as the heart of all the solutions throughout this study. It is the basis of the pH buffers as well as the environment for the bacteria detection. There are two reasons behind this. The first is because DI Water was seen to be much more stable for the SWNT sensors due to its lower resistance value. Second, the conductivity of the DI water is much more comparable to the conductivity of the pH buffers and the bacteria solutions allowing for a better understanding of the changes in impedance.

DI Water characterization also leads to an understanding of what happens on the surface of the SWNT film when the solution changes to pH and then bacteria. Between each test, DI water is re-tested in order to fully understand the affects of doping that occurs on the surface of the SWNT from dry state to wet state. The water surrounding the nanotubes that alters the electric field and dopes the pi network is believed to be a reversible doping affect. Once in wet state, the DI Water is now the base line of the remainder of the results conducted on the sensor. Prior to each test and after, all results are compared to the DI Water test in order to

conclude any further changes to the resistance or capacitance of the SWNT. From the wet state, the devices then undergo whole pH testing.

2.4.3 pH Sensing

Changing the solution that is being tested between various buffered solutions is the easiest way to study the variations that occur at the surface of the SWNT. When comparing larger capture biomolecules such as proteins and bacteria, that has varying charges along their primary structure, ions are small molecules of constant charge. A constant surface charge density can be achieved for SWNTs substrates by varying the pH of the solution. By controlling the electrostatic nature of the environment such as water to pH buffers to bacteria, comparison between different devices becomes straightforward and the specific sensing mechanism can be determined.

Research shows that pH solution change and its effect on CNT sensors like biomolecule sensing, has many of its own discrepancies. Literature shows that some research groups have reported an increase in conductivity with respect to an increase in pH levels.[107-109] However, on the other hand some researchers have observed an opposite trend where the conductivity decreases with an increase in pH levels.[110-114] Studies also show that a change in ionic strength also causes a shift in pH responses. Electron transfer after adsorption of H^+/OH^- ions is the most common explanation for these observed trends. Other reports on the opposite spectrum have even shown a no electrical change to bare nanotubes with pH change.[21] The explanation for the various trends and discrepancies can easily be related to the amount of possible defects present in the nanotubes as well as the several sensor fabrication methods. Based on the overall structure of the defective SWNTs, an opposite trend can easily be observed in comparison to the faultless tubes. Device fabrication steps involve many different surfactants, acid washes and cleaning processes that could all contribute to faulty interactions between SWNTs and the ions present in pH experiments. However, there is no clear indication as to why many different studies have reported contradictory pH dependent resistance responses. When it comes to the impedance of pH experiments on carbon nanotubes, the study of the change in capacitance and resistance is lacking. Some reports have shown that with an increase in pH levels, there is an increase in resistance. Studies have also reported that with an increase in ionic strength, resistance also tends to vary. Despite these findings, there has yet to be a detailed study on the impediametric response to pH changes that nanomaterials based biosensors undergo. This study however is a detailed experimental finding of how a SWNT based biosensor experiences changes in impedance,

specifically changes in resistance and capacitance with respect to change in pH levels as well as change in pH ionic strength.

A previous study conducted on SWNT based devices prior to SWNT based portable sensors has shown that SWNT based devices are in-fact ideal for real-time sensing. In this study, results show a time dependent I_d response to pH changes for a device at each aspect ratio at a constant V_d at 10mV. The conclusion for this study showed that SWNT devices did have a resistance dependence on solution pH and that the dominant sensing mechanism in this case is chemical doping. This study however required a further understanding of the changes in parameters when SWNT biosensors were subjected to environmental changes. **Figure 2.12** is a representation of the change that occurs when a SWNT biosensor was subjected to DI Water, followed by pH 4, 7 and 10 PB buffers through a microfluidic channel. It is a current vs. time graph that was conducted on a SWNT disposable substrate using a semi-conducting analyzer.

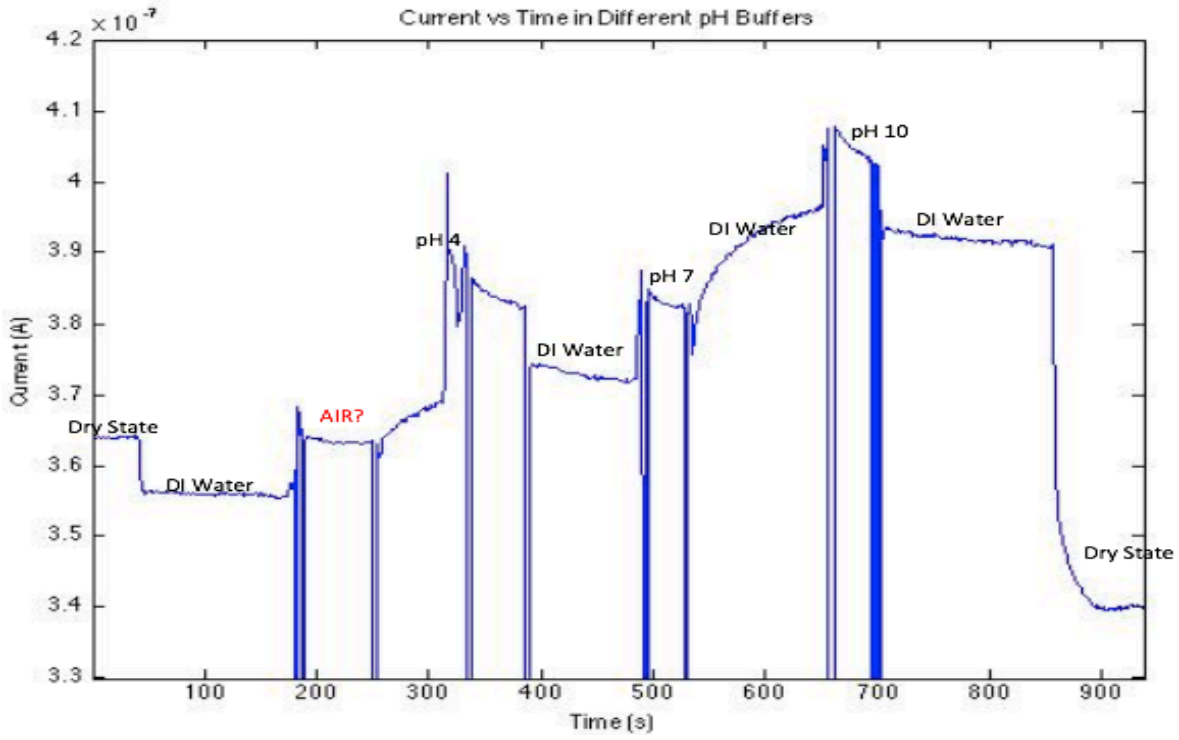

Figure 2.12: Time dependent current response to different pH conditions starting from Dry state, DI water and then pH 4, 7 and 10.

Figure 2.12 demonstrates that the SWNT device has a resistance dependence on solution pH. Beginning in dry state, a stable current is seen due to gasses in ambient conditions requiring very little time to arrange on the surface of the nanotube once a drain voltage is

applied. Once DI water is introduced, an instant decrease is observed in the drain current, which has been recognized as the water surrounding the nanotubes that is altering the electric field and doping the pi network of the SWNT.[21] After DI Water, pH 4 is introduced which can be seen to increase the resistance, followed by DI water again causing a decrease in resistance, followed by the same pattern for pH 7 and 10 with an increase in resistance every time. Theory behind this suggests that the reason for an increase in resistance with an increase in pH is most likely due to the doping affect of H^+/OH^- ions on the surface of the nanotubes. Although this test shows a significant amount of stability issues, this test clearly shows that the nanotubes are capable of immediately sensing an electrochemical change in their environment. In order to fix stabilization issues and to delete the noise that is experienced throughout the test, a much more stable solution was required. For this reason, building a set-up that will allow for almost zero noise, reproducibility, and a much deeper understanding of the changes in parameters experienced by these SWNT biosensors, a setup for electrochemical impedance measurements was completed.

The time dependent test shown in **figure 2.12** is a stabilized test that is conducted for pH sensing because of its immediate switch between H^+/OH^- ions on the surface of the nanotube that provides an instant kinetic response to change in resistance. This concept however is not the case for E.*coli* sensing. The antibody required for binding and the E.*coli* both have an incubation time of approximately 1hr, which once completed can only then undergo a response test. Due to this long incubation period, a kinetic test was not conducted as it would have not been a good representation between pH testing and bacteria sensing. Incubation times for bacteria and the binding time for antibody to the surface of the sensor can vary depending on the concentrations. A higher concentration would require a longer incubation time hence making it difficult for a kinetics test that can be similar to that of the pH testing. The impedance tests shown below for bacteria sensing however does show the difference between no incubation time followed by a 1hr incubation time.

Figure 2.13 is the exact test conducted above but instead of using a current vs time measurement to study the resistance change, an impedance measurement was taken. In this case instead of a 10mV current applied, only 5mV was required in order to achieve stable results. A consistent direction of resistance responses to pH change for device A and C can be seen in **figure 2.13.** There are a few things to take out of these results. The first is the stability of the sensors that can be seen from the smooth curve for DI Water, pH 4, 7 and 10. Second is the clear pattern that shows an overall increase in the total resistance with an

increase in pH level. It is also important to note that the conductivity of the buffered solutions was kept constant due to the phenomena that the conductivity directly affects the resistance. This can also be seen in **figure 2.13,** which shows that the R_s of DI Water is approximately 100 ohm, and has a conductivity of only 15uS. The R_s of the pH buffers is approximately double at 200 ohm, and has a conductivity of 7mS.

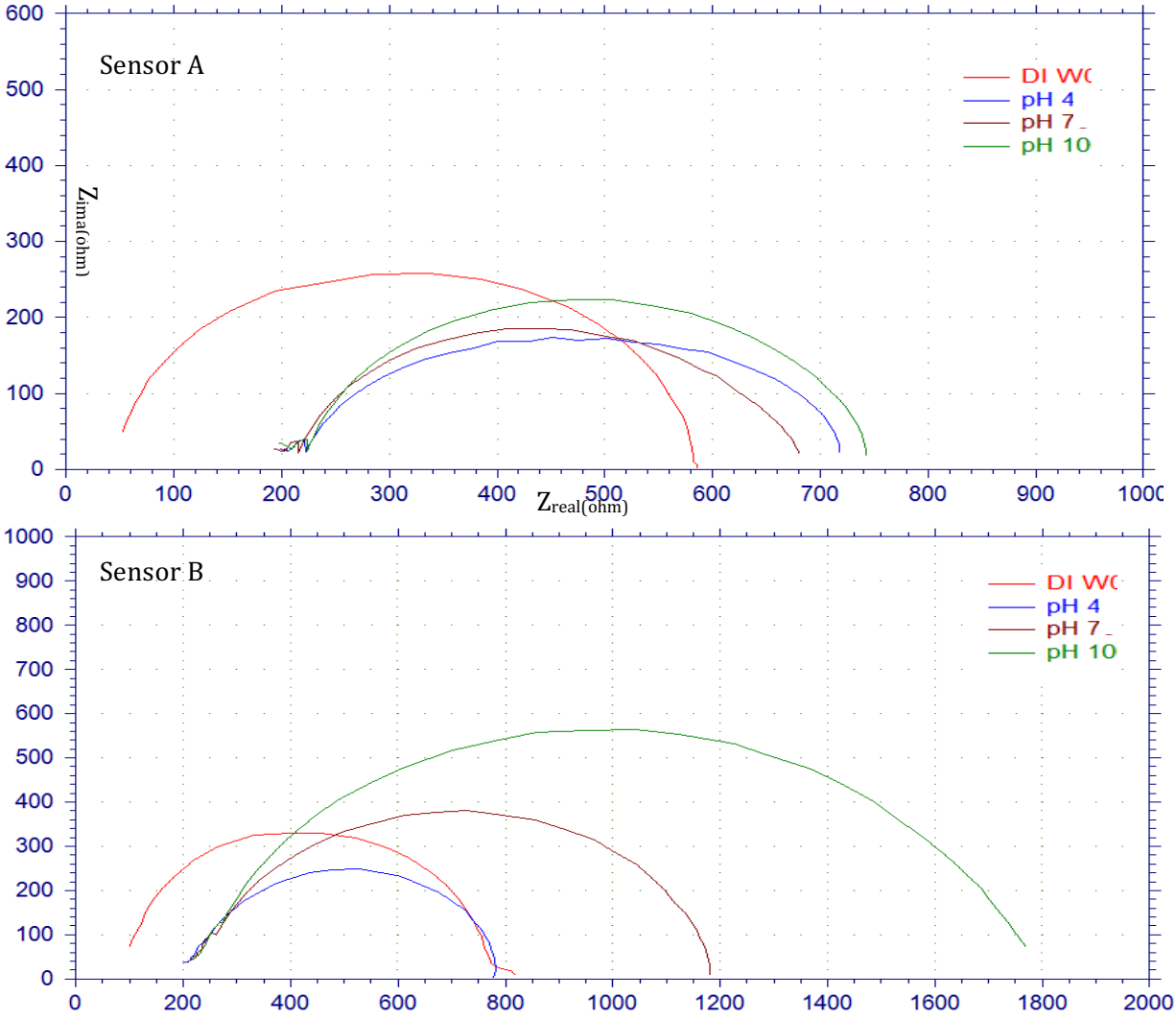

Figure 2.13: Impedance spectra of two devices with similar dry state resistance. Sensor a and b shows measurements taken during a DI water and pH test (Z_{real} (x-axis) vs Z_{img} (y-axis))

From **figure 2.13,** the first series of impedance tests conducted on SWNTs sensors, we were able to conclude that changes in environment does in-fact alter the change in impedance of the sensors. From the change in impedance we were able to calculate the change in solution resistance, charge transfer-resistance as well as the double layer capacitance of the SWNT sensor. The values for these parameters can be seen in **table 2.3** below. It is important to note that the dry state resistance for sensor A and B varies. Due to this variation, the R_s, R_{ct}, and C_{dl} values will also vary. The message to get out of these two graphs is the pattern that is observed when introducing DI water, pH 4, pH 7 and then pH 10. Despite the dry state resistance of these fabricated sensors varying from 1kohm to 2.8kohm, the response to the changes in the environment is always the same.

		R_s	R_{ct}	C_{dl}
Sensor A	**DI W**	51.68	519.8	4.412e-08
	pH 4	112.4	634.3	4.577e-06
	pH 7	87.38	576.8	1.695e-06
	pH 10	27.64	706.8	9.462e-07
Sensor B	**DI W**	101.6	658.8	2.584e-08
	pH 4	138.8	944	1.493e-07
	pH 7	130.6	1139.8	1.286e-07
	pH 10	127.6	1387	1.175e-06

Table 2.3: Solution resistances, Charge transfer resistance and double layer capacitance of Sensors A and B in solutions DI water, pH 4, 7 and 10.

Table 2.3 shows the values of three important parameters when studying the effects of the environment to SWNT biosensors. The pattern observed in this case indicates that the buffer solution resistance for both sensor A and B decreases from pH 4 to pH 10, however the solution resistance for DI water varies. The charge transfer resistance for sensor A increases from pH 4 to pH 10 but pH 7 replicates the charge transfer resistance similar to that of DI Water. For sensor B the charge transfer resistance for the pH buffers increases. In other words, the solution resistance decreases as the pH levels increase, but the charge transfer resistance increases as the pH levels increase. Therefore for the total resistance, the pattern observed is similar to what we see in literature that the total resistance increases as the pH levels increase. An interesting pattern was observed with the double layer capacitance with respect to an increase in ions present in the buffered solution. Although there were inconsistencies to this observation, the double layer capacitance tends to increase with an increase in pH level, corresponding to an increase in total capacitance, which in turn would increase the overall conductance of the SWNT. This can be seen in sensor B however sensor A shows less of a change. This could be due to the film difference between sensor A and B as well as the fact that conductivities were kept as constant as possible in order to understand the change in resistance to the SWNTs. Ideally, there shouldn't be much change in the double layer capacitance of the SWNT due to the fact that there are no additional ions present in solution but only a variance in H^+/OH^- ions. For this reasons, not observing a pattern for a chance in double layer capacitance agrees with theory and many literature reviews.

In order to understand the complete effect of pH levels on SWNT sensor resistance and capacitance, a much more detailed study was conducted that involved the full range of pH buffers. For these tests as well as for the basic test of DI Water, pH 4, 7 and 10, device fabrication was kept consistent. After conducting the basic DI water, pH 4, 7 and 10 tests to

ensure proper fabrication of the sensors and to rule out any faultiness of the sensors, pH buffers 5, 6, 8 and 9 were introduced in order to study the complete spectrum of pH level change with respect to resistance and capacitance. With the success of this test, we were able to conclude the sensing mechanism of the SWNT devices as well as the devices stabilization, and response amplification.

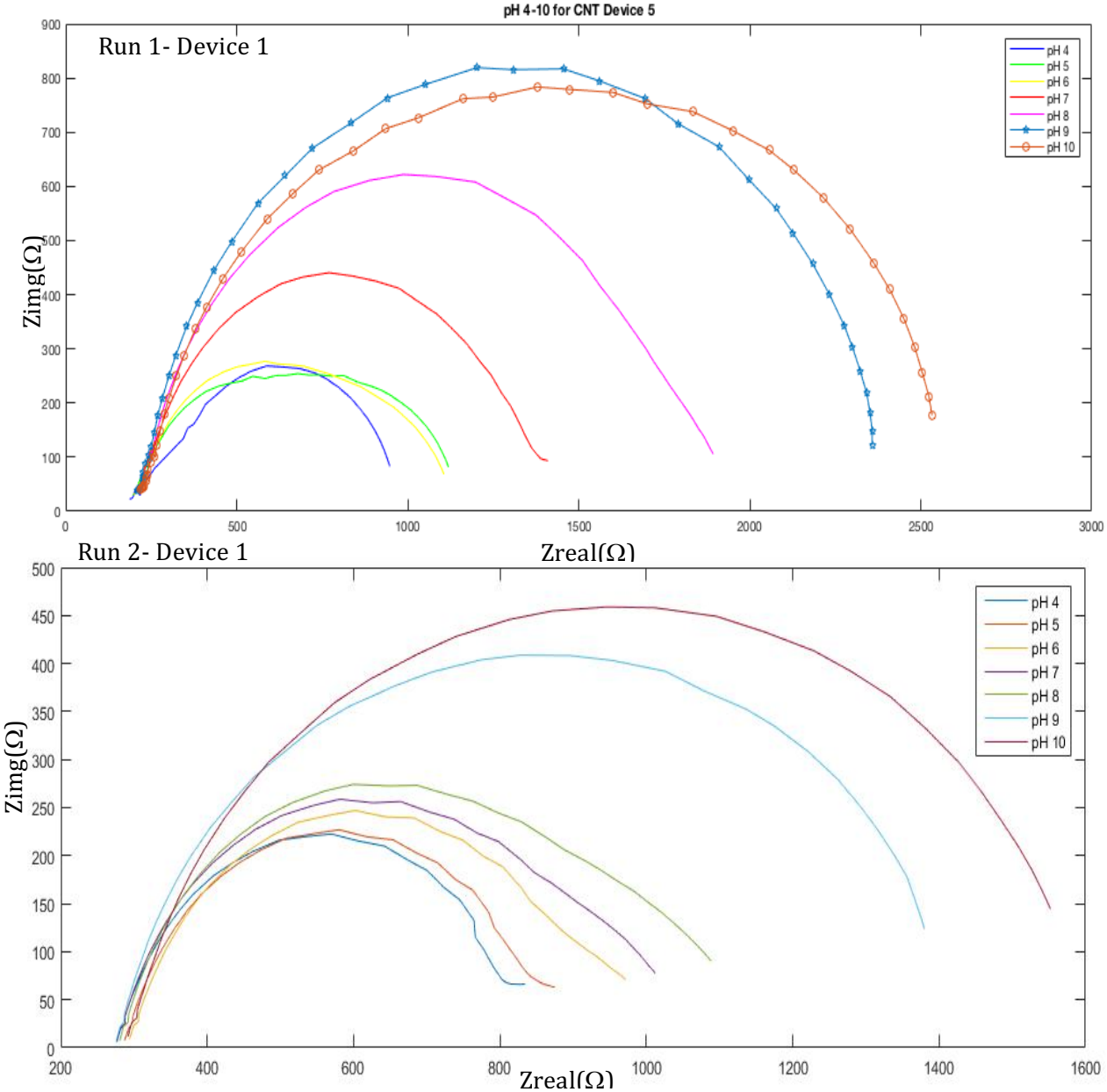

Figure 2.14: Representation of pH buffer levels 4-10 on SWNT Device 1. Run 1 is the test conducted in increasing order pH4 to 10 and Run 2 is the test conducted in reverse order from pH 10 to 4 (Z_{real} vs Z_{img})

Figure 2.14 run 1 and 2 and **figure 2.15** below shows the basic understanding of the effects of pH level increase with the total resistance of the SWNT. Between each pH level, the

sensor was washed with DI water in order to neutralize the sensor before the introduction of the next pH level. It can be seen that the R_s value of all the pH levels are almost identical indicating that the conductivity of the solutions are also alike. The R_{ct} of any impedance spectra is measured by the addition of the $R_{Au\ (electrode)} + R_{sens} + R_{anal}$. The resistance at the interface between the electrode and sensing layer is typically negligible. The measurement of R_{ct} requires the presence of redox-active species in the electrolyte. Although there are no redox reactions occurring in the solution but a simple electron transfer between OH^-/H^+, the R_{ct} value can be seen to increase from pH 4 to pH 10. This indicates that there is a shift in the ratio of H^+ ions to OH^- ions. It is important to note that the gap that is seen between pH 8 and 9 is consistent among all sensors however there is no explanation as to why this occurs. Moving on the total resistance ($R_s + R_{ct}$) as literature and these experiments have concluded, will increase with the increase in pH level. The stability of this test on the SWNT sensors was studied by reversing the introduction of the pH buffers to the surface. The reason for this was to prove that the surface of the SWNT was in fact responsive to the difference in OH^-/H^+ ions and not the simple idea of more being added to the surface. Run 2 in **figure 2.14** shows that even though pH 10 was the first buffer to be exposed to the SWNT and pH 4 was the last, the SWNT still behaves the same way as Run 1 and the electron transfer resistance responds in accordance to theory. The same pattern was observed where resistance increases with the increase in pH levels.

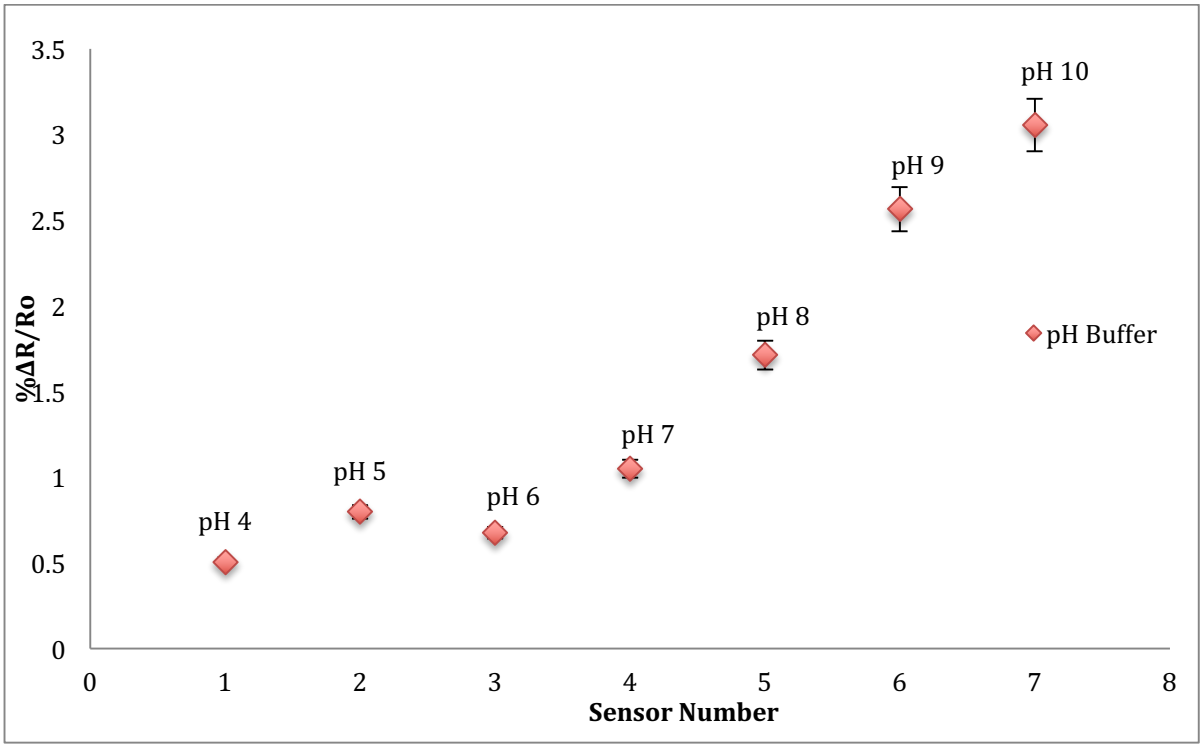

Figure 2.15: Representation of %ΔR/Ro with respect to change in pH level with an average of 5 runs per sensor. Each sensor in the x-axis corresponds to an average of 5 runs per a specific pH buffer. Sensor 1 was introduced with pH 4, sensor 2 introduced with pH 5, sensor 3 with pH 6, sensor 4 with pH 7, sensor 5 with pH 8, sensor 6 with pH 9, sensor 7 with pH 10.

2.4.4 Dominant Sensing Mechanism in SWNT Biosensors

The results shown in **figure 2.14** were conducted multiple times to ensure reproducibility, stability and the quality of the SWNT sensors. For confirmation of these properties for all the sensors fabricated, pH buffers 4, 7 and 10 were introduced prior to any further bacteria sensing. In addition to ensure proper fabrication of the sensors, it was observed that the introduction of the pH buffers chemically dopes the SWNTs, amplifying the signal of the test strips. Chemical doping is thought to be the dominant mechanism in pH response as $H^{=}/OH^{-}$ ions are adsorbed to the surface of the SWNTs. This involves partial electron transfer between a nanotube and charged molecules taking place at the nanotube's surface. Experiments have shown that resistance changes of the nanotube correspond to the redox state of the molecule in contact with the nanotubes rather than the overall charge of the molecule.[21] Being p-type in nature, nanotubes that interact with oxidizing molecules shown an increase in conductance resulting from depletion of the electros from the valence band, and vice versa for reducing molecules. This explains that $H^{=}$ adsorption occurring at

low pH levels resulting in a decreased network resistance while OH^- adsorption occurring at high pH levels resulting in an increased network resistance.

Section 1.3 has already proven that there are multiple proposed sensing mechanisms to explain and understand when it comes to electrical responses of SWNT based sensors that vary in electrochemical conditions. Between the two sensing mechanisms that were discussed, there lies a great deal of overlap that makes isolating the different mechanisms difficult. However, the main difference between the two sensing mechanisms that separates them from one another comes from the method of experimental sensing. When it comes to chemical doping, there is an adsorption of H^+/OH^- ions to the surface of the nanotube. This adsorption of ions corresponds to the experimental method used where the pH buffers are introduced to the surface of the nanotube for a certain period of time and then washed off. This on and off method allows for sensing to occur when the surface becomes chemically doped with the buffers. The method of electrostatic gating is slightly different. For this mechanism to be the primary sensing mechanism, there would be a charge build-up on a dielectric layer present on the SWNT with no direct contact with the SWNT, introduces an electrical potential that then shifts the fermi level of the SWNT. Since this is not the case experimentally, chemical doping is deemed to be the sensing mechanism over electrostatic gating. From the detailed study of pH buffers on SWNT devices in *section 2.3*, chemical doping is hence the dominant sensing mechanism. This may not be the case when it comes to bacteria sensing. A further study and explanation of the difference in the dominant sensing mechanism of pH sensing and bacteria sensing will be discussed in chapter 3.

Chapter 3: Bacteria sensing using disposable SWNT Biosensors

This chapter discusses the importance of real-time, point of care bacteria detection needs and the use of the previously mentioned fabricated SWNT disposable substrates for this demand. Chapter 1 and 2 illustrated that SWNTs are in-fact capable of real-time and ultrasensitive detection of bacteria and with this in mind, the aim of this project was to introduce Escherichia Coli (*E.Coli)* to the successfully fabricated SWNT substrates for real-time, point of care bacteria detection. In this study, fabricated SWNT sensors are treated with antibody reagents followed by blocking agents for elimination of non-specific binding, and then *E.coli* K-12. Surface modification in SWNT biosensors is specifically used so that there is a decrease in non-specific binding of the various molecules to the transducing component. In this work, antibody Anti-E.*coli* LPS specific for E.*coli* K12 MG1655 is immobilized to the surface. Triton X-100 is dispersed onto the SWNT's for protection of the SWNT's surface against non-specific binding of analyte to receptor molecules. Electrochemical impedance measurements are conducted on the prepared substrates and the change in resistance and capacitance with respect to change in solution environment is studied and reported below.

3.1 Introduction to bacteria sensing

Escherichia coli (E.coli), most commonly known as *E.coli,* refers to a large group of bacteria that is generally found in the intestines of humans and animals, typically through consumption of contaminated food or water. Most strains of *E.coli* are harmless, however strains such, as *E.coli* O157:H7 is the number one leading cause of diarrhea causing diseases leading to death worldwide.

Detection and monitoring of water or food borne pathogens are of utmost importance to the health and wellbeing of the general public. There exists a plethora of industries as well as individuals that will greatly benefit if disposable devices capable of real-time, sensitive, and selective detection of water- and foodborne pathogens are available to them. With the ability to determine whether current or potential sources of water are contaminated, individuals in developing countries can avoid ingesting diarrhea-causing bacteria such as *E. Coli*. Because this bacterium is the most common food and water borne pathogen, and the strains are easy to find, *E.coli* K-12 an isolate will be used as model for bacteria sensing.

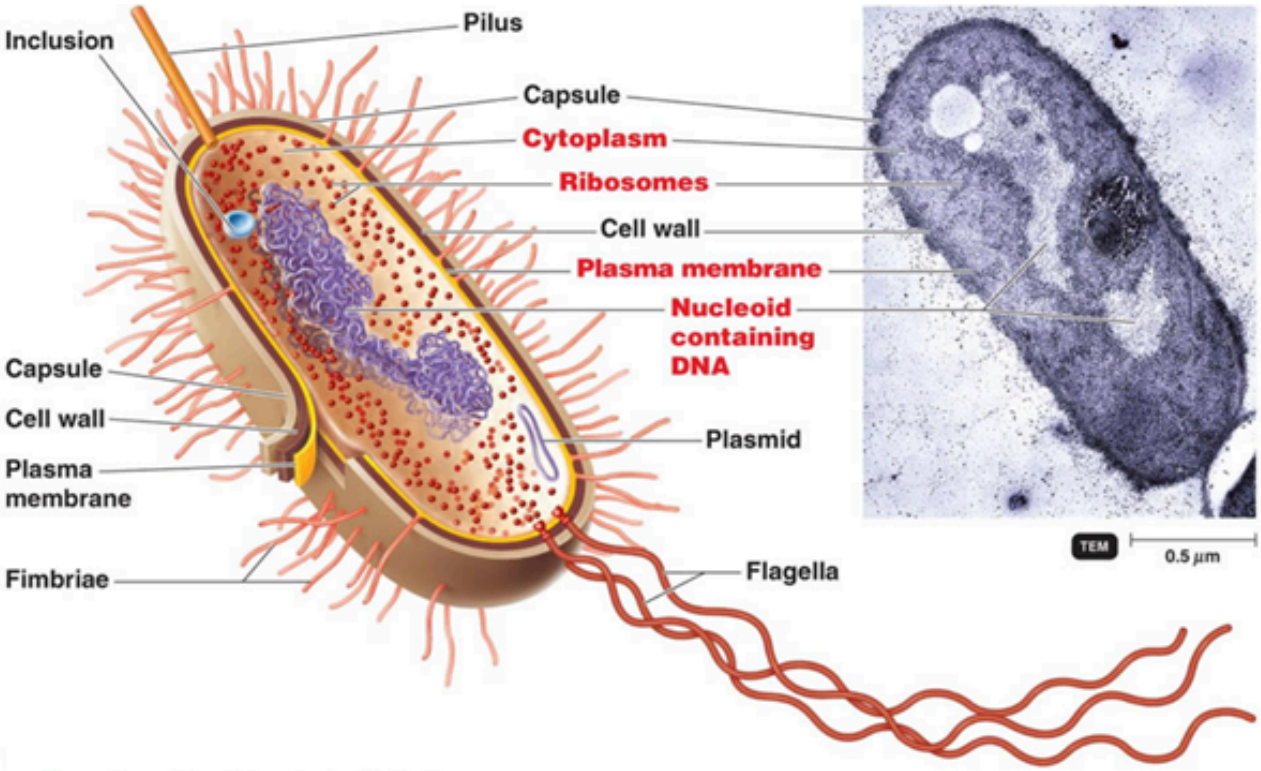

Figure 3.1: Schematic and TEM representation of *E.coli* bacterium used in this study.[115]

Figure 3.1 is a representation of what an *E.coli* bacterium looks like. It is important to notice the rod-shaped coliform bacterium that is normally found in the lower intestine of warm-blooded organisms. *E.coli* is expelled into the environment within fecal matter and the bacterium grows massively in fresh fecal matter under aerobic conditions for 3 days, but its numbers decline slowly as the days go one. The rod-shaped cells are typically about 2.0μm long and 0.25μm-1.0μm in diameters, with a cell volume of 0.6-0.7μm.[115] The bacterium can be grown and cultured easily and inexpensively in a laboratory setting, and has been intensively investigated for over 60 years. Optimum growth occurs at approximately 37°C and can grow in a variety of defined laboratory media such as lysogeny broth (LB broth), medium that contains glucose, or water.

With *E.coli* being the most studied prokaryotic model organism, where it has served as the host organisms for the majority of the work with DNA, it has taken the interest of many biotechnology studies. Because of its long history of laboratory culture and ease of manipulation, the use of *E.coli* in biotechnology studies has advanced. Specifically in the case of this study, *E.coli* K-12, a cultivated strain and well-adapted in the laboratory environment, is a strain that was isolated from a stool sample back in 1922 at Stanford University from a patient recovering from diphtheria.[115] Unlike wild-type strains, K-12, has lost its ability to

thrive in the intestine and is known to protect wild-type strains from antibodies and other chemical attacks. Because of this, by 1997, the entire genome of K-12 was sequenced. With this in-depth knowledge of K-12, many research groups have used K-12 for evolutionary experiments.

Using K-12 as the model for this study because of its simplicity in culturing and easy of manipulation, point of care, real-time sensing of bacteria can be accomplished. Point-of-care devices to date are limited to use in emergency rooms because of their sample volume requirements. Household devices on the other hand would allow for people to monitor their intake of samples that would contain such bacteria in order to confidently determine the likelihood of them becoming ill due to bacteria contamination. By allowing for this freedom of monitoring our own sample intake, the likelihood of bacteria caused illnesses would decrease significantly. The prevention of bacteria borne illnesses would not only save many lives, but also save money and time from individuals filling up the ER. This type of monitoring inherently calls for disposable, cost-efficient, real-time sensors that are capable of bacteria detection. With this in mind, the prototype shown in chapter 2 was carried over and introduced to bacteria sensing. After proving its success to changes in DI water and pH levels, the potential of portable SWNT biosensors increases significantly.

3.2 Fabrications and Method

The aim of this project was to realize a disposable SWNT sensor that is capable of detecting cfu/mL concentrations of bacteria. The fabrication process for the SWNT sensor is identical to that of the SWNT biosensor studied in chapter 2. In addition to pH sensing, bacteria sensing simply requires the immobilization of antibodies to the surface of SWNT in order to eliminate non-specific binding.

The method used to immobilize the antibodies to the surface of the SWNT is discussed in chapter 1. Through non-covalent binding, the antibodies are adsorbed to the surface of the SWNT after an hour of incubation. After incubation, the SWNT sensor is washed using DI water in order to eliminate any unbound antibodies and then nitrogen dried. Prior to blocking, an impedance spectrum is taken to ensure complete saturation of the antibody to the surface of the SWNT. Anti-*E.coli* LPS was the antibody used for *E.coli* K-12. After antibody immobilization, blocking agent Triton X-100 is dispersed on the surface of SWNT for approximately 1 hr. This process ensures that only specific binding occurs between receptor and analyte molecules on the surface of the SWNT. After the two steps, the substrate is prepared and ready for bacteria immobilization.

3.3 Results and Discussion

3.3.1 *E.coli* K-12 Sensing

With all the previous characterization completed, the SWNT test strips were then used to test various concentrations of K-12. The receptor molecule chosen in this case as mentioned previously is Anti-*E.coli* LPS specific for the strain of bacteria used in this study K-12 MG1655. In addition to the original K-12 stock, pGlo glycerol was added to the culture in order to visualize the bacteria cells under fluorescence. It is important to note that the addition of pGlo does not alter the size or shape of the bacteria in any way and therefore does not alter the results obtained in these experiments.

The sensing aspect of the test arises from the attachment of the bacteria cells by measuring the change in electrical properties of the sensor due to the insulating properties of the SWNT. A response is taken prior to each immobilization step because of the theory that each additional intact to the electrodes effectively reduces the electrode area that the current reaches and hence increases the interface impedance, and thus determines the resulting sensor signals. By measuring the impedance between each immobilization step, a comparison from the prior step is studied in order to determine any changes to the surface. **Figure 3.2** below shows the affects that each step has on the surface of the SWNT after DI water and pH characterization. A very important factor that must be taken into account when testing each response of these test strips is their real-time response. The end goal of the project was to fabricate a device capable of real-time sensing of bacteria present in water. If the sensor is not able to detect changes to the surface almost immediately or within minutes, the practicality of these devices is diminished. **Figure 3.2** shows the response of the SWNT test strips to a change in solution environment as well as to the change in surface immobilization.

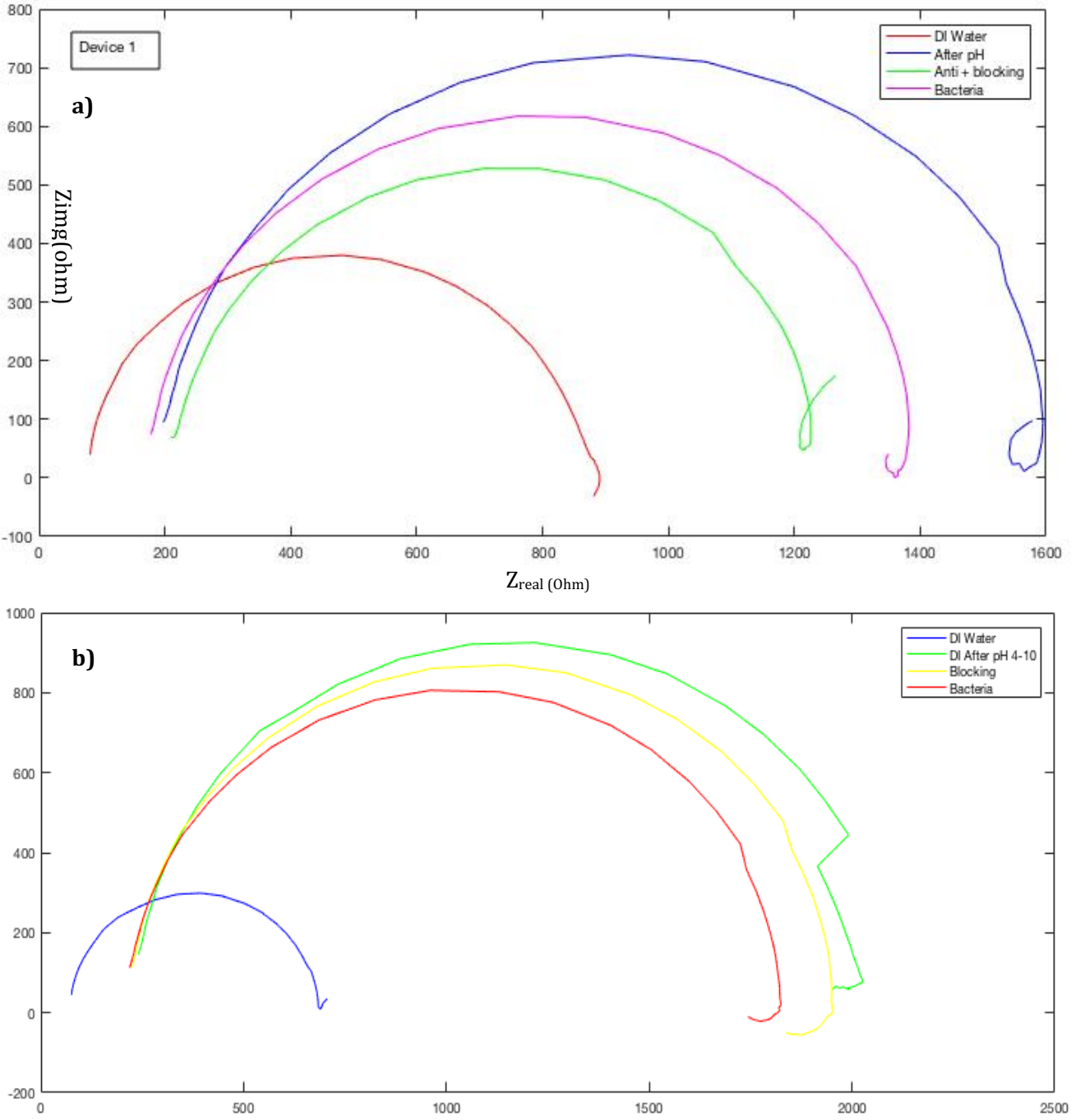

Figure 3.2: Real-time (Z_{real} vs Z_{img}) response with respect to different immobilization steps of the SWNT sensors. a) DI Water, pH buffers, antibody, blocking and 10^5 cfu/mL e.coli and b) DI Water, DI Water after pH buffers, and 10^5 cfu/mL e.coli

The graphs shown in **figure 3.2** show the results of the real-time Z_{real} vs Z_{img} impedance of two different scenarios. **Figure 3.2a)** is the positive control of bactria detection using 10^5 cfu/mL as a preliminary run in order to determine the effects of antibody to surface

immobilization and antibody to bacteria binding. The first step of this test involved the introduction of DI water with an instantaneous response time, followed by pH buffers 4, 7 and 10, Antibody and blocking, and then bacteria. There are a few things that can be concluded from this test. The first is the confirmation of chemical doping occurring on the surface of the SWNT. The second is that the antibody + blocking immobilization is successful by seeing an increase in resistance by adding to the surface of the SWNT and lastly bacteria detection, which is also seen to cause an increase in total resistance of the SWNT sensor. With an increase in resistance after each step, the results are directly related to what theory suggests that immobilization on the surface increases the charge transfer resistance each time. **Table 3.1** shows the difference in R_s, $R_{ct,}$ and C_{dl} of the different steps in bacteria sensing. **Figure 3.2b)** is the negative control of the bacteria detection shown in a. In this case following the same protocol except with the elimination of the antibody step, it can be seen that the bacteria does not bind to the surface of the SWNT but that without the immobilization of the antibody to the surface, bacteria is lost and the resistance decreases. This confirms that antibody immobilization is indeed occurring on the surface of the SWNT and the resistance of the SWNT is increasing for each step. **Table 3.2** shows the resistance and capacitance values for this test.

Device #	DI Water	DI after pH 4/10	Anti + Blocking	Bacteria
1 (1.665)	R1= 80.85 R2= 773.9 C2= 5.374e-08	R1= 216.6 R2= 1539 C2= 2.745e-08	R1= 214.6 R2= 1025 C2= 6.267e-08	R1= 177.3 R2= 1229 C2= 3.63e-08

Table 3.1: Representation of the values for figure 3.2a) where R1= R_s, R2=R_{ct}, and C2=C_{dl}

	DI Water	pH Buffers (4-10)	Blocking	Bacteria
Device 5	R1= 74.37 R2= 608.9 C2= 4.548e-08	pH 4: R1= 91.58 R2= 937.8 C2= 6.473e-06 pH 7: R1= 279.8 R2= 1120 C2= 1.232e-06 pH 10: R1= 1074 R2= 1687 C2=5.636e-06	R1=222.5 R2=1741 C2=2.306e-08	R1=220.8 R2=1604 C2=2.325e-08

Table 3.2: Representation of the values for figure 3.2b) where R1= R_s, R2=R_{ct}, and C2=C_{dl}

The equivalent circuit for the data presented above is identical to the equivalent circuit mentioned in chapter 2. It consists of the resistance (R_s) of the electrolyte between the electrodes, the charge or electron-transfer resistance (R_{ct}) and the double layer capacitance (C_{dl}). The R_s represents the properties of the bulk solution and since the bulk solution is kept constant, they are not affected by the changes occurring on the surface of the electrodes. In this case, the other two elements R_{ct} and C_{dl}, depend on the dielectric and insulating features as the electrode/electrolyte interface, and they are affected by the cell attachment at the electrodes surface.

The charge transfer resistance is the parameter measured in the immunosensor. Theory suggests that the attachment of the bacterial cells to the sensor surface increases the electron transfer resistance. The total charge transfer resistance after cell attachment can be expressed as:

$$R_{ct} = R_c + R_{cell}$$

Where R_c and R_{cell} are the charge transfer resistance of the antibody immobilized electrode and the variable charge transfer resistance introduced by the attached bacterial cells. From the nyquist plots shown in **figure 3.2**, extrapolation of the semi-circle yields that the diameter of the semicircle is equal to the charge-transfer resistance. **Figure 3.2** shows the nyquist plot of the bare SWNT sensor in DI Water, after antibody immobilization and after *E.coli* K-12. The charge transfer resistances (the diameters of the semicircle and values shown in **table 3.1**) increase each step. The R_{ct} of the electrode after antibody immobilization and cell binding was 774Ω, 1025Ω, and 1229Ω, respectively. This result demonstrated that the charge-transfer resistance is a feasible parameter to measure the change on the electrode surface due to immobilization of antibodies and the binding of *E.coli* K-12. Without antibody immobilization as shown in **table 3.2**, the R_{ct} value does not share the same increasing pattern as it does with the antibody immobilization.

The equivalent circuit model also involves the double layer capacitance and theory suggests that there should be a change in C_{dl} when there is an increase in cell depth. With the attachment of antibodies and bacteria to the cell, theoretically there should be a change in C_{dl} however this is not the case. The measured capacitance usually arises from the series combination of several elements, such as analyte binding to a sensing layer, on an Au electrode. In this case the capacitance is measured by the following for a sensing layer and analyte layer that are continuous.

$$\frac{1}{C_d} = \frac{1}{C_{Au}} + \frac{1}{C_{sens}} + \frac{1}{C_{anal}}$$

In many cases, the capacitance at the electrode-sensing layer interface is significantly large and can be neglected. The sensitivity is then determined by the relative capacitance of the analyte layer and the sensing layer.[116] For each dielectric layer, the capacitance per unit area depends on the layer thickness (t) according to:

$$\frac{C}{A} = \frac{\varepsilon_d}{t}$$

where ε_d is the dielectric constant of the dielectric layer and so capacitance and most sensitive to binding of large analytes, such as proteins and bacteria. The difficulty with capacitance and a reason why it is difficult to get a change in value can be due to the fact that their sensitivity depends on obtaining proper thickness of the original sensing layer. With the variation in SWNT thickness in addition to the antibody and bacteria immobilization, the sensitivity of the electrode surface varies each time. If the original sensing layer is too thin, then the underlying electrode surface may be partially exposed, which allows for non-specific interactions from interfering species. However, in the opposite case where the original sensing layer is too think, then the AC impedance current that is detected is dramatically reduced, as is the change in capacitance upon analyte binding. Theoretically in the case of this experiment, capacitance should increase with the addition of the antibody and large bacteria cells however this is not observed in any case. In-fact, almost no change in capacitance is observed when it comes to bacteria sensing. Most studies have spent their time and research in the resistance parameter over the capacitance and this could be due to the significant complications that lie within the double layer capacitance of biosensors.

After confirmation of successful 10^5cfu/mL detection of K-12, preliminary results have shown that the possibility of lower concentration of bacteria can be detected and comparable only if the SWNT deposited on the substrate is identical to the others. A difference in thickness of the tubes will alter the results of bacteria. **Figure 3.3** is a representation of the preliminary results of bacteria sensing from 10^2-10^5 cfu/mL. The pattern observed for these results differs from the results presented in **figure 3.2**. In this case, the resistance was observed to have minimal to almost no change but the double layer capacitance indicates that there is an increase with increase in analyte concentration. The reason behind this phenomenon could indicate that instead of the bacteria adding thickness to the sensing layer, the addition of bacteria to the nanotube in-fact removes the immobilized antibodies. The increase in capacitance in this case can be from the electrode surface rather than the SWNT double layer.

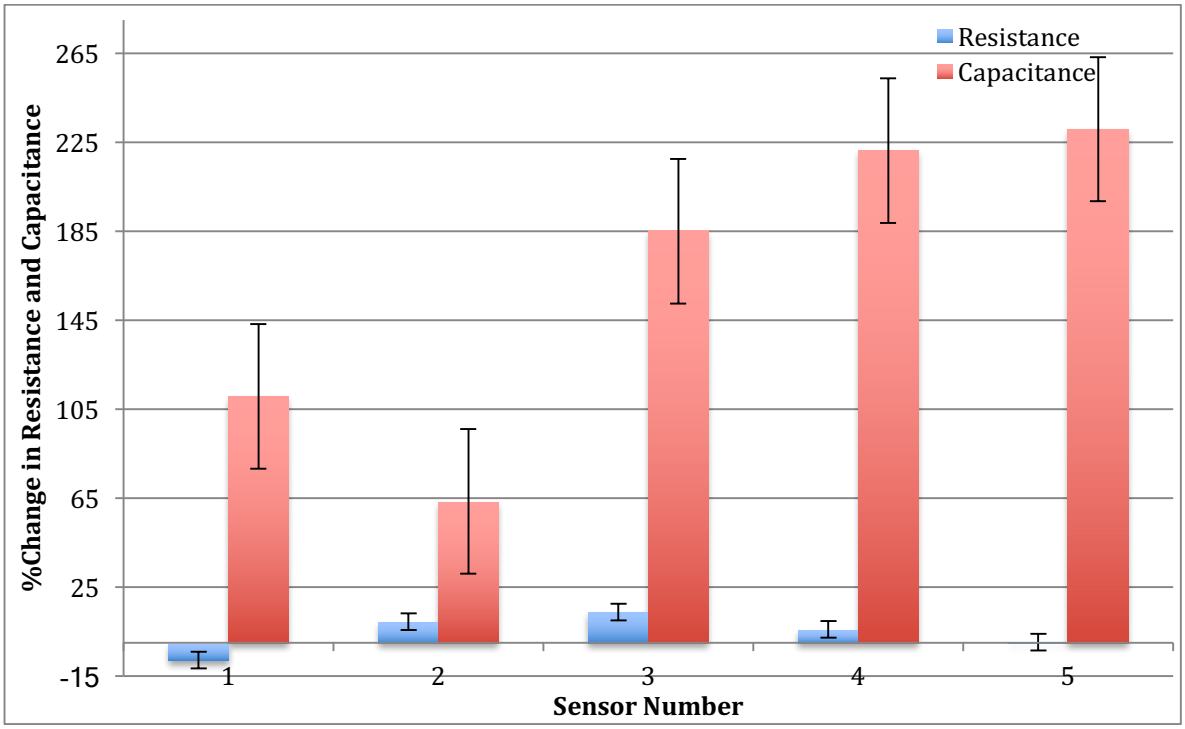

Figure 3.3: Representation of the preliminary data for K-12 sensing of concentrations 10^2-10^5cfu/mL. Graph shows sensor number with respect to change in resistance and capacitance. Sensor 1 is DI Water with no bacteria, sensor 2 DI Water spiked with 10^2 cfu/mL of bacteria , sensor 3 is 10^3 cfu/mL, sensor 4 is 10^4 cfu/mL and sensor 5 is10^5cfu/mL.

The results shown in **figure 3.3** is a clear indication that more study needs to be done in order to determine the change in resistance and capacitance caused by the a difference in analyte concentration. Previous data indicated that there should be a visible change in resistance with respect to change in analyte concentration as well as a change in double layer capacitance with a change in analyte concentration. This however is not the case when it comes to decreasing the concentration of bacteria. 10^5cfu/mL was the successful limit of detection for this study but a much more detailed understanding of the double layer capacitance is required before decreasing the concentration of bacteria.

Theoretically, with a change in analyte concentration and surface immobilization such as antibodies binding to the surface of the nanotube, there should be a clear indication for a change in resistance and change in double layer capacitance between each step. For instance, with an attachment of antibodies to the surface of the nanotube, the resistance should have increased from bare state. From antibody immobilization, the resistance should have increased again when bacteria was introduced and successfully bound to the antibodies. This was not the case when conducting bacteria detection. There are a few reasons as to why this could be the case. The first involves the possibility of the antibody not binding to the surface

of the nanotubes. Without a strong binding between the antibodies to the surface of the nanotube, the wash stages between detection steps could potentially wash away the antibodies. There were no tests conducted to determine whether or not antibody surface immobilization was successfully completed. An electrochemical test did determine a change in resistance but not enough to conclude that this change was in fact due to antibody surface immobilization. This step of antibody to surface binding is an ongoing study and with the conclusion of this process, bacteria detection would be much easier to understand.

Chapter 4: Conclusions and Future Work

4.1 Conclusions

This work demonstrates the reproducibility of CVD grown SWNTs used as the transducing component in chemiresistive biosensors. The study involves confirming the underlying sensing mechanism of the SWNT based biosensor and the effects of dry state electrical properties as well as their sensing capabilities were studied.

Device analysis demonstrates that chemical doping was the dominant sensing mechanism of sensing as pH levels change. The surface sites available for H^+/OH^- adsorption as well as the ion's reducing/oxidizing nature are the principle reasons for this conclusion. Further it was observed that as the pH buffer levels increased, the total resistance also increased. This study was conducted in reverse to ensure that the principle reason behind this change was based on the difference in H^+/OH^- adsorption sites. These results also concluded that no matter what order of pH levels, the total resistance increases with an increase in pH levels.

Fabrication of cost-effect, disposable, real-time and sensitive SWNT biosensors on PET substrates is realized through the conclusion of this work. Using impedance methods for the detection of bacteria, this study was able to conclude that surface immobilization of bare electrodes, to antibody and then bacteria changes the resistance and capacitance of the sensor. The charge transfer resistance of the SWNT biosensor increased with the addition of surface immobilization. From a bare electrode in DI Water, to antibody immobilization and bacteria immobilization, the charge transfer resistance had a linear response and increases every time. A detection limit of 10^5 cfu/mL was observed using the fabricated SWNT biosensors. The preliminary results for a limit of detection lower than 10^5cfu/mL indicates that there is a removal of antibody and bacteria from the surface. Electrical tests show an increase in double layer capacitance but no pattern in resistance. Further experimentation is required to confirm these preliminary results.

4.2 Future Work

Future work is required for the results seen in *section 3* **figure 3.3.** This is because the results shown in this section do not agree with the results shown in previous sections and is opposite to what was expected when conducting multiple concentrations of the SWNT biosensors. With a further in depth study of what happens on the surface of the SWNT when introduced to bacteria, optimization of the SWNT test strip can take place and a lower limit of detection could enhance the ability of these test strips. A further understanding of the double layer capacitance is also required. Studies indicate that the double layer capacitance should change with respect to resistance change for bacteria detection however this was not the case. The resistance for bacteria sensing below 10^5cfu/mL also did not have the expected pattern.

Although there was a successful response from the devices to the antibody immobilization followed by the 10^5cfu/mL, a further study on this concentration would provide a better understanding as to why there was no observed change in the double layer capacitance there from the DI water to antibody to bacteria. These results did show a good understanding to the change in resistance with respect to literature review but there is no clear understanding as to what goes on with the double layer capacitance.

Future work should also involve another method of determining what is happening on the surface of the SWNTs when they undergo surface immobilization. Fluorescent visualization would be ideal where counting the bacteria cells that are stuck to the surface of the SWNT can confirm whether or not the electrical response is in fact coming from the antibody to bacteria binding and not somewhere else.

4.3 Summary

The main goal of this was to demonstrate the capabilities of SWNT chemiresistive biosensors and to fabricate a disposable, real-time point of care substrate that is capable of detecting bacteria. In order to achieve this, successful fabrication and characterization of two different platforms was required. The first allowed for the effects of pH and *E.coli* K-12 sensing abilities and the underlying sensing mechanism, and the second was the commercialization of the SWNT chemiresistive biosensor.

Successful pH sensing was accomplished using the SWNT disposable substrate in order to confirm the underlying sensing mechanism. Chemical doping was determined to be the dominant sensing mechanism during the pH tests of bare carbon nanotubes. pH testing confirmed that with an increase in pH levels, the resistance of the SWNT substrate also increases.

Detection of 10^5 cfu/mL *E.coli* K-12 was also accomplished using the same SWNT portable biosensors. Antibody immobilization was deemed successful with an increase in charge transfer resistance followed by a successful detection of 10^5 cfu/mL of K-12. Impedance studies for biosensing applications have proven to be a very good tool in determining the effects of surface change electrochemically. Impedance techniques were able to determine change s occurring on the surface of the SWNT almost immediately via electrochemically. These results proved that the sensitivity of the SWNT biosensor that can be used for the detection of bacteria lower than 10^5 cfu/mL and therefore allowing for a successful fabrication of a portable SWNT device that is in real-time, point of care and disposable.

References

1. Joseph, W., Carbon nanotube based electrochemical biosensor. *Analytical Chem.* **17**, 7-14 (2005)

2. Veetil, J. V & Ye, K. Development of Immunosensors Using Carbon Nanotubes. *Biotechnol. Prog.* **23,** 517-531 (2007)

3. Nie, S. M., Emery, S. R., Probing single molecules and single nanoparticles by Surface-Enhanced Raman Scattering. *Science,* **275,** 1102 (1997)

4. Lu, H., Xun, L., Xie, X., Single-molecule enzymatic dynamics. *Science,* **282,** 1877 (1998)

5. Feigel, I., Vedala, H., Biosensors based on one-dimensional nanostructures. *J. Mater. Chem.* **21,** 8940-8954 (2011)

6. Dantham, V. R. *et al.* Label-Free Detection of Single Protein Using a Nanoplasmonic-Photonic Hybrid Microcavity. *Nano Lett.* **13,** 3347–3351 (2013)

7. He, L., Ozdemir, S. K., Zhu, J., Kim, W. & Yang, L. Detecting single viruses and nanoparticles using whispering gallery microlasers. *Nat. Nanotechnol.* **6,** 428–32 (2011)

8. Vollmer, F., Arnold, S. & Keng, D. Single virus detection from the reactive shift of a whispering-gallery mode. *Proc. Natl. Acad. Sci. U. S. A.* **105,** 20701–20704 (2008)

9. Washburn, A. L., Luchansky, M. S., Bowman, A. L. & Bailey, R. C. Quantitative, Label-Free Detection of Five Protein Biomarkers Using Multiplexed Arrays of Silicon Photonic Microring Resonators. *Anal. Chem.* **82,** 69–72 (2010)

10. Zhu, H., White, I. M., Suter, J. D., Zourob, M. & Fan, X. Opto-fluidic micro-ring resonator for sensitive label-free viral detection. *Analyst* **133,** 356–360 (2008)

11. Huang, M. J. *et al.* Serotype-Specific Identification of Dengue Virus by Silicon Nanowire Array Biosensor. *J. Nanosci. Nanotechnol.* **13,** 3810–3817 (2013)

12. Huang, Y.W. *et al.* Real-Time and Label-Free Detection of the Prostate-Specific Antigen in Human Serum by a Polycrystalline Silicon Nanowire Field-Effect Transistor Biosensor. *Anal. Chem.* **85,** 7912–7918 (2013)

13. Patolsky, F. *et al.* Electrical detection of single viruses. *Proc. Natl. Acad. Sci. U. S. A.* **101,** 14017–22 (2004)

14. Shirale, D. J. *et al.* Label-free chemiresistive immunosensors for viruses. *Environ. Sci. Technol.* **44,** 9030–5 (2010)

15. Tuan, C. Van, Huy, T. Q., Hieu, N. Van, Tuan, M. A. & Trung, T. Polyaniline Nanowires-Based Electrochemical Immunosensor for Label Free Detection of Japanese Encephalitis Virus. *Anal. Lett.* **46,** 1229–1240 (2013)

16. Vidic, J. *et al.* Surface Plasmon Resonance Immunosensor for Detection of PB1-F2 Influenza A Virus Protein in Infected Biological Samples. *J. Anal. Bioanal. Tech.* **S7,** 1–7 (2013)

17. Wang, S. *et al.* Label-free imaging, detection, and mass measurement of single viruses by surface plasmon resonance. *Proc. Natl. Acad. Sci. U. S. A.* **107,** 16028–32 (2010)

18. Yakes, B. J. *et al*. Surface plasmon resonance biosensor for detection of feline calicivirus, a surrogate for norovirus. *Int. J. Food Microbiol.* **162,** 152-158 (2013)

19. Lazcka, O., Javier Del Campo, F., Xavier Munoz, F., Pathogen detection: A perspective of traditional methods and biosensors. *Biosen. and Bioelec.* **22**, 1205-1217 (2007)

20. Bergveld, P. Development of an ion-sensitive solid-state device for neurophysiological measurements. *IEEE Trans. Biomed. Eng,* **BME-17,** 70-71 (2013)

21. Ward, A., A study of mechanisms governing single walled carbon nanotube thin film electric biosensors. *Unpublished master's thesis,* 4-6 (2013)

22. Luo, X. & Davis, J. J. Electrical biosensors and the label free detection of protein disease biomarkers. *Chem. Soc. Rev.* **42,** 5944–62 (2013)

23. Feigel, I. M., Vedala, H. & Star, A. Biosensors based on one-dimensional nanostructures. *J. Mater. Chem.* **21,** 8940–8954 (2011)

24. Kurkina, T., Label-free electrical biosensing based on electrochemically functionalized carbon nanostructures. *Thesis dissertation,* 14-17 (2012)

25. Zhang, G.-J. & Ning, Y. Silicon nanowire biosensor and its application in disease diagnostics: a review. *Anal. Chim. Acta* **749**, 1-5 (2012)

26. Nair, P. R. & Alam, M.A. Screening-limited response of nanobiosensors. *Nano Lett.* **8,** 1281-1285 (2008)

27. Nair, P. R. & Alam, M. A. Dimensionally Frustrated Diffusion towards Fractal Adsorbers. *Phys. Rev. Lett.* **99,** 256101 (2007)

28. Lee, K., Nair, P. R., Scott, A., Alam, M. a. & Janes, D. B. Device considerations for development of conductance-based biosensors. *J. Appl. Phys.* **105,** 102046 (2009)

29. Yang, W., Ratinac, K. R., Ringer, S. P., Thordarson, P., Gooding, J., Braet, F. Carbon Nanomaterials in Biosensors: Should you use nanotubes or graphene? *Angew. Chem. Int. Ed.* **49,** 2114-2138 (2010)

30. Kocabas, C., Shim, M., Rogers, J.A., Spatially selective guided growth of high-coverage arrays and random networks of single-walled carbon nanotubes and their integration into electronic devices. *J. Am. Chem. Soc.* **128**, 4540-4541 (2006)

31. Jacobs, C., Peairs, M., Venton, B., Review: carbon nanotube based electrochemical sensors for biomolecules. *Anal. Chem. Acta* **662**, 105-127 (2010)

32. Tey, J. N., Wijaya, I. P. M., Wang, Z., Goh, W. H. & Palaniappan, A. Laminated, microfluidic-integrated carbon nanotube based biosensors. *Appl. Phys. Lett.* **94,** 013107 (2009)

33. Liu, Y., Li, X., Dokmeci, M. R. & Wang, M. L. Carbon Nanotube Sensors Integrated Inside a Microfluidic Channel for Water Quality Monitoring. *Sensors Smart Struct. Technol. Civil, Mech. Aerosp. Syst.* **7981,** 1–8 (2011)

34. Nair, P. R., Alam, M. A. Performance limits of Nanobiosensors. *Apps. Phys. Lett.* **88,** 9-11 (2006)

35. Garcia-Aljaro, C., Cella, L., Shirale, D., Park, M., Munoz, FJ., Yates, MV., Mulchandani, A. Carbon nanotubes-based chemiresistive biosensors for detection of microorganisms. *Biosens. Bioelectron.* **26**(4), 1437-41 (2010)

36. Dong, B. X. *et al.* Electrical Detection of Femtomolar DNA via Gold-Nanoparticle Enhancement in Carbon-Nanotube-Network Field-Effect Transistors. *Adv. Mater.* **20,** 2389–2393 (2008)

37. Lee, D., Chander, Y., Goyal, S. M. & Cui, T. Carbon nanotube electric immunoassay for the detection of swine influenza virus H1N1. *Biosens. Bioelectron.* **26,** 3482–7 (2011)

38. Aqui, L., Yanez-Sedeno, P., Pingarron, J. Role of carbon nanotubes in electroanalytical chemistry: a review. *Anal Chem Acta*. **622,** 11-47 (2008)

39. Pumera, M., Sanchez, S., Ichinose, I., Tanj, J. Electrochemical nanobiosensors. *Sens. And Act.* **123,** (2007)

40. Rao, C., Satishkumar, B., Govindaraj, A., Nath, M. Nanotubes. *Chem. Phys. Chem.* **2**, 78-105 (2001)

41. Ward, A., Petrie, A., Honek, J., Tang, X., Analyte dependent sensing mechanisms governing single walled carbon nanotube thin film biosensors. *IEEE Nano. Tech. Mag.* **8,** 29-37 (2014)

42. Novoselov, K., Geim, A., Morosov, S., Jiang, D., Zhang, Y., Dubonos, S., Grigorieva, I., Firsov, A. Electric Field effect in atomatically thin carbon films. *Sci.* **306,** 666-9 (2014)

43. Ajayan, P., Nanotubes of Carbon. *Chem. Rev.* **99,** 1787-99 (1999)

44. Torres, L., Roche, S., Charlier, J.C. Introduction to Graphene-Based Nanomaterials: From Electronic Structure to Quantum Transport. *Contem. Phys.* **4,** 344-45 (2014)

45. Jariwala, Z., Sangwan, K., Lauhon, L., Marksab, T., Hersam, M. Carbon nanomaterials for electronics, optoelectronics, photovoltaics, and sensing. *Chem. Soc. Rev.* **42,** 2824 (2013)

46. Iijima, S. Helical microtubules of graphitic carbon. *Nature.* **356,** 56-58 (1991)

47. Dresselhaus, M., Dresselhaus, G., Saito, R. Physics of carbon nanotubes. *Carbon.* **33,** 883-891 (1995)

48. Britz, D. and Khlobystov, A., Noncovalent interactions of molecules with single walled carbon nanotubes. *Chem. Soc. Rev.* **35,** 637-659 (2006)

49. Huang, J. Atomic structure and electronic properties of single-walled carbon nanotubes. *Nat.* **391,** 1997-99 (1998)

50. Franklin, D., Luisier, S., Han, G., Tulevski, C., Breslin, L., Gignac, M., Haensch, W. Flexible Electronics: From Materials to Devices. *Nano Lett.* **12**, 758–762 (2012)

51. Skulason, E. Metallic and Semiconducting properties of Carbon Nanotubes. *Mod. Phys.* **2,** 8-21 (2005)

52. Minot, E. Tuning the band structure of carbon nanotubes. *Ph.d Thesis,* 15-21, (2004)

53. Saito, R., Fujita, G., Dresselhaus, G., Dresselhaus, M. Electronic structure of chiral graphene tubules. *App. Phys. Lett.* **60,** 2204-2206 (1992)

54. Endo, M., Hayashi, T., Kim, Y. Large-scale production of carbon nanotubes and their applications. *Pure App. Chem.* **78,** 1703-1713 (2006)

55. Charlier, J. C. Electronic and transport properties of nanotubes. *Rev. Mod. Phys.* **79**, 677-732 (2007)

56. Gruner, G. Carbon nanotube transistors for biosensing applications. *Anal. Bioanal. Chem.* **384**, 322-335 (2006)

57. Ajayan, P. Functionalization of carbon nanotubes and other nanocarbons by azide chemistry. *Chem. Rev*. **99**, 1787 (1999)

58. Yu, X., Munge, B., Patel, V., Jensen, G., Bhirde, A., Gong, JD., Kim, SN., Gillespie, J., Gutkind, JS., Papadimtrakopoulos, F. and Rusling, JF. Carbon nanotube amplification strategies for highly sensitive immunodetection of cancer biomarkers. *J. Am. Chem. Soc.* **128,** 11199-11205 (2006)

59. Heller, I., Kong, J., Heering, H., Williams, K.A., Lemay, S.G., Dekker, C. Individual single-walled carbon nanotubes as nanoelectrodes for electrochemistry. *Nano Lett*. **5,** 137-142, (2005)

60. Hiura, H., Ebbesen, T. W., Tanigaki, K. Opening and purification of carbon nanotubes in high yields. *Adv. Mat.* **7,** 275-276 (1995)

61. Kurkina, T., Balasubramanian, K. Towards in vitro molecular diagnostics using nanostructures. *Cell Mol Life Sci.* **69,** 373-88 (2012)

62. Krapf, D., Quinn, B., Wu, M.-Y., Zandbergen, H.W., Dekker, C., Lemay, S.G. Experimental observation of nonlinear ionic transport at the nanometer scale. *Nano Lett.,* **6,** 2531-35 (2006)

63. Gooding, J., Chou, A., Liu, J., Losic, D., Shapter, J., Hibbert, D. The effects of the lengths and orientations of single-walled carbon nanotubes on the electrochemistry of nanotube-modified electrodes. *Electro. Comm.,* **9,** 1677-1683 (2007)

64. Guiseppi-Elie, A., Lei, C., Baughman, R. Direct electron transfer of glucose oxidase on carbon nanotubes. *Nanotech.,* **13,** 559 (2002)

65. Chen, Z., Tabakman, S.M., Goodwin, A.P., Kattah, M.G., Daranciang, D., Wang, X., Zhang, G., Li, X., Liu, Z., Utz, P.J., Jiang, K., Fan, S. and Dai, H. Protein microarrays with carbon nanotubes as multicolor Raman labels. *Nat. Biotechnol*. **26,** 1285-1292 (2008)

66. Alwarappan, S., Erdem, A., Liu, C., Li, C.Z. Probing the electrochemical properties of graphene nanosheets for biosensing applications. *J. Phys. Chem.* **113,** 8853-57 (2009)

67. Yu, X., Munge, B., Patel, V., Jensen, G., Bhirde, A., Gong, J.D., Kim, S.N., Gillespie, J., Gutkind, J.S., Papadimtrakopoulos, F. and Rusling, J.F. Carbon nanotube amplification strategies for highly sensitive immunodetection of cancer biomarkers. *J. Am. Chem. Soc.* **128,** 11199-11205 (2006)

68. Balasubramanian, K., Burghard, M. Biosensors based on carbon nanotubes. *Anal. Bioanal. Chem.* **385,** 452-468 (2006)

69. Sotiropoulou. S., Chaniotakis, N.A., Carbon nanotube array-based biosensor. *Anal Bioanal. Chem.* **375,** 103-105 (2003)

70. Yu, X., Chattopadhyay, D., Galeska, I., Papadimitrakopoulos, F., Rusling, J.F. Peroxidase activity of enzymes bound to the ends of single-wall carbon nanotube forest electrodes. *Electrochem. Comm.* **5,** 408-411 (2003)

71. Gruner, G. Carbon nanotube transistors for biosensing applications. *Anal. Bioanal. Chem.* **384,** 322-335 (2006)

72. Collins, P.G., Bradley, K., Ishigami, M., Zettl, A. Extreme oxygen sensitivity of electronic properties of carbon nanotubes. *Science*. **287,** 1801-1804 (2000)

73. Besteman, K., Lee, J-O., Wiertz, F.G.M., Heering, H.A., Dekker, C. Enzyme-Coated Carbon Nanotubes as Single-Molecule Biosensors. *Nano Lett.* **3,** 727-730 (2003)

74. Star, A., Tu, E., Niemann, J., Gabriel, J-CP., Joiner, C.S., Valcke, C. Label-free detection of DNA hybridization using carbon nanotube network field-effect transistors. *Proc. Natl. Acad. Sci.USA.* **103,** 921–926 (2006)

75. Maehashi, K., Matsumoto, K., Takamura, Y., Tamiya, E. Aptamer-based label-free immunosensors using carbon nanotube field-effect transistors. *Electroanal.* **21,** 1285-1290 (2009)

76. Fam, D. W. H., Palaniappan, A., Tok, a. I. Y., Liedberg, B. & Moochhala, S. M. A review on technological aspects influencing commercialization of carbon nanotube sensors. *Sensors Actuators B Chem.* **157,** 1–7 (2011)

77. Tans, S. J., Verschueren, A. R. M. & Dekker, C. Room-temperature transistor based on a single carbon nanotube. *Nature* **393,** 49–52 (1998)

78. Martel, R., Schmidt, T., Shea, H. R., Hertel, T. & Avouris, P. Single- and multi-wall carbon nanotube field-effect transistors. *Appl. Phys. Lett.* **73,** 2447–2449 (1998)

79. Heller, I. *et al.* Identifying the Mechanism of Biosensing with Carbon Nanotube Transistors. *Nano Lett.* **8,** 591–595 (2008)

80. Salehi-khojin, A. *et al.* On the Sensing Mechanism in Carbon Nanotube Chemiresistors. *ACS Nano* **5,** 153–158 (2011)

81. Nair, P. R. & Alam, M. A. Performance limits of nanobiosensors. *Appl. Phys. Lett.* **88,** 233120 (2006)

82. Heller, I., Janssens, A.M., M, J., Minot, E.D., Lemay, S.G., Dekker, C. Identifiying the Mechanism of Biosensing with Carbon Nanotube Transistors. *Nano. Lett.* **8,** 591-595, (2007)

83. Fam, D., Palaniappan, A., Tok, I., Liedberg, B., Moochhala, S.M. A review on technological aspects influencing commercialization of carbon nanotube sensors. *Sens. Act. B.* **157**, 1-7 (2011)

84. Artyukhin, A.B., Stadermann, M., Friddle, R.W., Stroeve, P., Bakajin, O., Noy, A., Controlled electrostatic gating of carbon nanotube FET devices. *Nano. Lett.* **6**, 2080-2085 (2006)

85. Fischer, J.E. Chemical Doping of Single walled carbon nanotubes. *Acc. Chem. Res.* **35,** 1079-1086 (2002)

86. Zahab, A., Spina, L., Poncharal, P. & Marliere, C. Water-vapor effect on the electrical conductivity of a single-walled carbon nanotube mat. *Phys. Rev. B* **62,** 0–3 (2000)

87. Larrimore, L., Nad, S., Zhou, X., Abruña, H. & McEuen, P. L. Probing electrostatic potentials in solution with carbon nanotube transistors. *Nano Lett.* **6,** 1329–1333 (2006)

88. Li, X., Guard, L. New doping method improves electronic properties of carbon nanotubes. (2016)

89. Young, M. E., Carroad, P. A. & Bell, R. L. Estimation of Diffusion Coefficients of Proteins. *Biotechnol. Bioeng.* **22,** 947–955 (1980)

90. Schoning, M., Poghossian, A. Recent advances in biologically sensitive field-effect transistors. *Anal.* **127***,* 1137-1151 (2002)

91. Karch, H., Tarr, P., Bielaszewska, M. Enterohaemorrhagic *Escherichia coli* in human medicine. *Int. J. Med. Microbiol.* **295**, 405–18 (2005)

92. Thomas, M.K., Murray, R., Flockhart, L., Pintar, K., Fazil, A., Nesbitt, A., Marshall, B., Tataryn, J., Pollari, F. Estimates of foodborne illness-related hospitalizations and deaths in Canada for 30 specified pathogens and unspecified agents. *Foodborne Pathog. Dis.* **12,** 820-827 (2015)

93. Chaib, F., WHO's first ever global estimates of foodborne diseases find children under 5 account for almost one third of deaths. *www.who.int/foodborne-disease-estimates. World Health Org.* (2015)

94. Ahmed, A., Rushworth, J., Hirst, N. Biosensors for Whole-Cell Bacterial Detection. *Clin Microbiol Rev.* **27**, 631-646 (2014)

95. Martinez MT., Tseng YC., Ormategui N., Loinaz I., Eritja R., Bokor J. Label-Free DNA Biosensors Based on Functionalized Carbon Nanotube Field Effect Transistors. *Nano Letters*. **9**, 530–536 (2011)

96. Malig J., Englert JM., Hirsch A., Guldi DM. Wet Chemistry of Graphene. *Interface*. **20**, 53-56 (2011)

97. Jeng ES., Moll AE., Roy AC., Gastala JB., Strano MS. Detection of DNA Hybridization Using the Near-Infrared Band-Gap Fluorescence of Single-Walled Carbon Nanotubes. *Nano Letters.* **6,** 371–375 (2006)

98. Rushworth JV., Hirst NA., Goode JA., Pike DJ., Ahmed A., Millner PA. Impedimetric biosensors for medical applications: current progress and challenges. *ASME* (2013)

99. Kuriyama T., Kimura J. FET-based biosensors. Bioprocess Technol. **15**, 139-162 (1991)

100. Besteman K., Lee J-O., Wiertz FGM., Heering HA., Dekker C. Enzyme-Coated Carbon Nanotubes as Single-Molecule Biosensors. *Nano Lett.* **3,** 727-730 (2003)

101. Heller I., Janssens AM., Männik J., Minot ED., Lemay SG., Dekker C. Identifying the mechanism of biosensing with carbon nanotube transistors. *Nano Lett.* **8,** 591-595 (2008)

102. Lindholm-Sethson B, Nyström J, Malmsten M, Ringstad L, Nelson A, Geladi P. Electrochemical impedance spectroscopy in label-free biosensor applications: multivariate data analysis for an objective interpretation. *Anal Bioanal Chem.* **398**, 2341-2349 (2010)

103. Pethig, R., Smith, S. Introductory Bioelectronics for Engineers and Physical Scientists. *Wiley.* **3**, 278-283 (2013)

104. Ahmed, A., Rushworth, J.V., Hirst, N., Millner, P. Biosensors for Whole-Cell Bacterial Detection. *Clin Microbiol Rev.* **27**, 631-646 (2014)

105. Ishikawa, F. N. et al. Importance of controlling nanotube density for highly sensitive and reliable biosensors functional in physiological conditions. *ACS Nano.* **4**, 6914-6922 (2010)

106. Rose, K., Kelly, D., Kemker, C., Fitch, K., Card, A. Fundamentals of environmental measurements. *Fondriest.com. Fon. Environ. Inc.* (2016)

107. Back, J. H. & Shim, M. pH-dependent electron-transport properties of carbon nanotubes. *Phys. Chem. B* **110**, 23736–23741 (2006)

108. Haeberle, T. et al. Solution processable carbon nanotube network thin-film transistors operated in electrolytic solutions at various pH. *Appl. Phys. Lett.* **101,** 223101 (2012)

109. Heller, I. et al. Influence of electrolyte composition on liquid-gated carbon nanotube and graphene transistors. *J. Am. Chem. Soc.* **132,** 17149–17156 (2010)

110. Munzer, A. M. et al. Back-gated spray-deposited carbon nanotube thin film transistors operatrd in electrolytic solutions: an assessment towards future biosensing applications. *J. Mater. Chem*. **1,** 3797–3802 (2013)

111. Li, P., Martin, C. M., Yeung, K. K. & Xue, W. Dielectrophoresis aligned single-walled carbon nanotubes as pH sensors. *Biosensors* **1**, 23–35 (2011)

112. Lee, D., Cui, T. & Member, S. Layer-by-Layer Self-Assembled Single-Walled Carbon Nanotubes Based Ion-Sensitive Conductometric Glucose Biosensors. *IEEE Sens. J.* **9,** 449–456 (2009).

113. Chien, Y.-S. et al. The pH Sensing Characteristics of the Extended-Gate Field-Effect Transistors of Multi-Walled Carbon-Nanotube Thin Film Using Low-Temperature Ultrasonic Spray Method. *J. Nanosci. Nanotechnol.* **12,** 5423–5428 (2012).

114. Wu, Z. et al. Transparent, Conductive Carbon Nanotube Films. *Science (80-).* **305,** 1273–1276 (2004).

115. Bachmann, B. Pedigrees of some mutant strains of Escherichia coli K-12. *Bacterio. Rev.* **36,** 525-557 (1972)

116. Suni, I. Impedance methods for electrochemical sensors using nanomaterials. *Anal. Chem.* **27,** 604-611 (2008)

Appendix A- Fabrication

A.1.1- Single Walled Carbon Nanotubes

The procedure for synthesizing SWNTTFs begins with the preparation of a catalyst solution. Firstly, 7nm silica nanoparticles are loaded with catalyst metals. This is done by dissolving 50mg of silica powder as well as 3.0mg of Iron (III) acetylacetonate, 0.7mg of Molybdenum (II) acetate and 4.6mg of Cobalt (II) acetate in two separate vials containing 10mL of ethanol. The solutions are then sonicated for 30 minutes and then mixed together. Once mixed, the solution is sonicated for an additional 2 hours. Sonication at this time promotes the impregnation of the catalyst metals into the pores of the silica nanoparticles. This is an important step as the duration of sonication determines the overall how well dispersed the nanoparticles are in solution which in turn controls the film's homogeneity. Once the catalyst is prepared, it can be diluted in order to control the density of the film.

Silicon/2μm SiO_2 (thermal) wafers are used as the growth substrates. Prior to coating the substrate with catalyst, the wafers are cleaned using RCA 1 protocol. This is done in order to remove any contaminants from the surface of the wafer and ensure that the SiO_2 surface is hydroxylated. The catalyst is able to completely and constantly wet the surface of the wafer when there are OH groups present. The diluted catalyst is then pipetted onto the surface of the wafer. The wafer is then spun at 2500rpm for 1 minute then immediately placed on a hot plate at 120°C for 5 minutes. Chemical vapor deposition is then used to grow the SWNTTF. The substrate is then placed into a 2in quartz tube CVD chamber in a high purity Argon (1200 sccm) and Hydrogen (36 sccm) environment. The temperature of the tube furnace is then ramped to the growth temperature of 850°C. Once the growth temperature is reached the flow of gas is diverted through an ethanol bubbler held at -1°C for 20min. The bubbler is then bypassed and the chamber is allowed to cool to room temperature.

A.1.2- SWNT Liftoff, Transfer, Patterning and Cleaning

In order to make use of the CVD grown SWNTTFs they must be transferred onto the electrode array. The film is then hand etched into 2mm x 8mm rectangles that will be transferred onto the patterned electrodes. As the films are grown on and anchored onto a 2μm layer of SiO_2, a hydrofluoric acid bath is capable of wet etching the oxide layer to facilitate liftoff. The wafer is placed in a 5% HF in DI H_2O for approximately 20 seconds and swiftly placed into a DI H_2O bath very slowly. The film is capable of free standing on the surface of the water due to its hydrophobic nature and the surface tension of water. Using a pre-patterned Au substrate, the SWNT film is lifted off the surface of the water and allowed to dry at room temperature to minimize wrinkling in the film.

A.2- PET Based SWNT Devices

The fabrication of the PET based devices begins with preparing purchased glucose sensing test strips (Accuchek Aviva test strips, Hoffmann La Roche, Ltd.). Figure A.4 shows the progression of the PET based test strips.

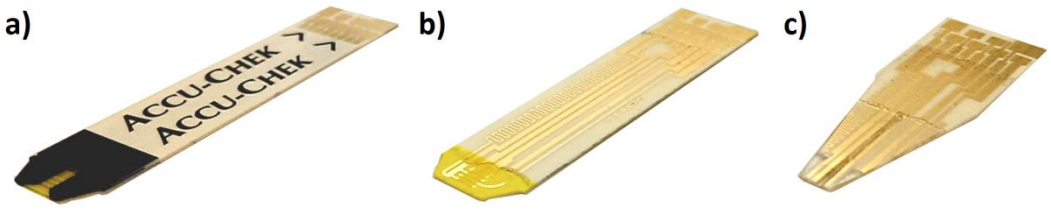

Figure A.4: Images concerning complete PET device fabrication including a) purchased test strip, b) stripped from original packaging and c) final device after removal of acrylic adhesive

Figure A.4 depicts the simple approach taken to realize a fully functional SWNTTF chemiresistor. Beginning with the purchased test strip figure A.4(a), simply peeling the top cover off of the test strip gives access to the patterned gold electrodes and glucose-oxidase coated region seen in figure A.4(b). The area used for glucose sensing is then cut off and left

over adhesive is then removed by rubbing the electrodes in an ethanol bath. A patterned SWNT is then transferred into the region between two adjacent electrodes. The electrodes are then covered with an acrylic adhesive (McMaster Carr, Ltd), to control the exposed surface area, which can be seen as the final test strip prototype in figure A.4(c).